Reply to Referee Comments for manuscript acp-2018-482 by Pascal Graf, Heini Wernli, and Harald Sodemann: A new interpretative framework for below-cloud effects on stable water isotopes in vapour and rain

Comments of the referees are in *italics;* our replies are in normal font.

We thank both reviewers for their comments, which helped to clarify the manuscript. The originally submitted version lacked a clear explanation of the effects of kinetic fractionation and its influence on Δδ and Δd. Thus, in our substantially revised version we decided to include and discuss the results of idealised simulations with a below-cloud interaction model to illustrate the influence of different atmospheric parameters on the location of precipitation samples in the ΔδΔd-space. As a consequence, we include Stephan Pfahl as a co-author in the revised manuscript.

Comments of referee 1

Answers on general comments:

1. *There is significant ignorance of the theory of kinetic fractionation. In case of unsaturated condition, there is always kinetic fractionation occurring during either evaporation or isotopic exchange. Equilibrium fractionation is defined in case of saturated condition.*

REPLY: We did not ignore kinetic fractionation. While there are several passages in the text where this is highlighted (P3, L.1; P8, L.10, P8, L.17, P8, L. 20), we acknowledge that we did not mention its influence clearly enough, in particular on Δδ and Δd. We outline below how kinetic fractionation is related to Δδ and Δd, and improve the relevant descriptions in the manuscript:

We agree that kinetic fractionation occurs in unsaturated conditions. In addition, kinetic fractionation occurs in saturated conditions when vapour and precipitation are far from their equilibrium composition, i.e., in the presence of large gradients for a single isotope species. The latter case is however usually ignored when qualitatively interpreting isotope data because the effects are small. Equilibrium fractionation in contrast occurs during both saturated and unsaturated conditions. The total fractionation during unsaturated conditions is then a combination of equilibrium and kinetic/non-equilibrium fractionation. We define Δδ and Δd as the difference between ambient vapour and equilibrium vapour of precipitation. Under saturated conditions, given enough time, this difference becomes 0‰ due to equilibration. In unsaturated conditions, equilibration also acts to reduce Δδ and Δd, it is however counteracted and often outweighed by the effect of non-equilibrium fractionation, which increases Δδ and decreases Δd.

2. *In the present paper, the situation of Δδ=Δd=0 occurred when RH<100%. That means, the situation did not happen because the vapour and liquid were in equilibrium state. Rather than that, it was occurred by kinetic fractionation process depending on specific RH and the initial dD and d18O values of vapour and liquid.*

REPLY: The situation Δδ=Δd=0‰ at RH<100% indeed does not occur when vapour and rain have enough time to interact. Evaporation will increase Δδ and decrease Δd and, if strong compared to equilibration, move the rain sample away from Δδ=Δd=0‰. Thus, when falling through unsaturated air, precipitation must have had a negative Δδ and a positive Δd in order to arrive at the surface at Δδ=Δd=0‰. We agree that the situation probably did not occur because they were in a state of equilibrium. However, arriving at the surface with Δδ=Δd=0‰ excludes strong evaporation, for which a strongly positive initial Δd would be necessary, which is not realistic (cf. P9, L11-14). More realistic is either a saturated column, except for the lowermost layer, where RH was measured, or precipitation obtained a positive Δd by equilibration with vapour aloft, with a higher d_v than vapour at the surface.

3. *The kinetic fractionation would behave quite complicatedly in Δδ Δd diagram, according to Stewart's (1975) formulation, which is the most popular parameterization in the isotope general circulation models, for example, Δδ and Δd are highly sensitive to the initial isotopic values of rain and vapor and RH of the ambient air. On the other hand, "the degree of equilibration" would not make such a big difference in Δδ Δd diagram. As stated above, there is always kinetic fractionation occurring in unsaturated condition, so if such*

kinetic fractionation's final state is practically called "equilibrium" (by the way, this is what is parameterized in the most of the models, e.g., Hoffmann et al., 1998; Yoshimura et al., 2008), this equilibration would not always become $\Delta\delta=\Delta d=0$, because there is kinetic fractionation process going on.

REPLY: We want to first clarify how we use the term equilibration. By equilibration we mean the exchange of isotopes between vapour and rain in saturated air. In unsaturated air, we assume that this equilibration is the same and acts along the same direction, but it is complemented by evaporation, which makes the final trajectory of a sample in the ΔδΔd-space different. The final trajectory is the sum of the vectors of pure equilibration and evaporation (the length of the vectors depends on the intensity of the processes). This combination would not always cause samples to move to $\Delta\delta=\Delta d=0$‰, as you state correctly, it would move them to 'kinetic fractionations final state' or what Stewart (1975) described with δ_{end} (his Eq. 3c).

Kinetic fractionation is part of the evaporation process and acts along a well-defined direction in the ΔδΔd-space when separated from the equilibration process, i.e., when RH=0%. Using Stewart's approach, the slope of the direction along which evaporation acts is around –1.3 +/– 0.4 $\Delta d/\Delta\delta$ with dependencies on the delta-value, temperature and on which fraction of the initial drop is remaining (see Fig. A in this reply document). The difference for varying conditions is thus not very large. Evaporation always acts towards the bottom right of the ΔδΔd-diagram. Equilibration without evaporation (RH=100%) however, does indeed depend strongly on the isotopic difference between equilibrium vapour from precipitation and vapour ('local' Δδ and Δd, see answer to P2 of reviewer 2). At the surface, equilibration acts towards the origin (0,0), denoting the composition of near-surface vapour in the ΔδΔd-diagram.

Thus, the trajectories of pure equilibration and evaporation act in very different directions in the ΔδΔd-space, which helps to separate their influence. The final location of a sample in the ΔδΔd-diagram is then an interplay of the initial composition and its modification by evaporation and equilibration. Since we can constrain the initial composition by a certain extent (P9, L10 onwards), and because we know the directions into which equilibration and evaporation act, we can deduce information about the relative importance of below-cloud processes from the location of a sample in the ΔδΔd-space. In the revised version, we will add a discussion of these factors to Sec. 5 and the Conclusions, using also results from the idealized simulations with the below-cloud interaction model.

4. *This ignorance of kinetic fractionation processes significantly influences the interpretation of the paper. For example, P9L17 "Strongly equilibrated sample are thus located close to the origin" is probably misleading. That is true when RH=100%, but not true when RH<100%. P9L21 "Rain samples that are strongly affected by evaporation will thus be located in the bottom right quadrant" may be misleading too. It is highly depended on initial condition and RH, and different initial condition and RH may cause different trend in evaporation line in $\Delta\delta\Delta d$. So, the right bottom position would not be reflected by "stronger evaporation".*

REPLY: We agree that the formulation can appear too strong and lead to misinterpretation. We rephrased these sentences as follows: Strongly equilibrated samples *tend* to be located close to the origin. They can also be there due to other reasons, such as specific initial conditions. However, initial conditions have a limited range of realistic values. Samples without evaporation are therefore unlikely to be located in the bottom right corner. Samples from highly intense rain and a low melting layer will not be located close to the origin and samples from very light rain and high saturation will not be located in the bottom right or on the left of the ΔδΔd-diagram, because the initial conditions necessary for this to happen are not realistic. In the revised manuscript, we include a set of sensitivity experiments with a below-cloud fractionation model to explore a range of realistic variation in the ΔδΔd-space.

Answers to specific comments:

P2L16: Did the authors come across any new understanding of below-cloud processes?

REPLY: We show that by means of a new interpretation framework for below-cloud processes using stable isotopes, the effect of equilibration and evaporation on precipitation below the cloud can (to some extent) be separated. In addition, we identify the role of key factors during a frontal passage, including boundary-layer humidity, precipitation intensity and melting layer height. As an example, this was stated in item 4 of the

conclusions as "Post-frontal samples are less equilibrated and evaporated than pre-frontal samples, due to higher below-cloud relative humidity and a lower temperature and melting layer after the frontal passage." Our study paves the ground for further work which can employ this framework in different weather situations. We will emphasize these aspects even more clearly in the abstract and conclusions of the revised manuscript.

P8L8: What is "cloud signal"?

REPLY: By 'cloud signal' we refer to the initial composition of precipitation after formation, which is governed by the isotopic composition of the cloud vapour (amongst other influences like the temperature during formation and the formation mechanism). We adapted the text in order to clarify:
"Data points to the left of the origin indicate that precipitation is more depleted than ambient air, and reflect that more of the initial signal after formation ("cloud signal") is retained in precipitation"

P8L12: More explanation for the other three events are necessary. Another big issue of the paper is lack of observation data. Are the characteristic of cold fronts similar? How about temporal tendency of the evaporation strength?

REPLY: The other three events are presented in detail in Graf (2018). Including them in this manuscript with proper consideration of the measurement setup, data treatment, meteorological description and interpretation would go beyond its scope. We do not understand the comment about a lack of observations data, given that a unique detailed data set of the frontal transition in terms of high-resolution vapour and precipitation isotope measurements with 86 samples are used in this manuscript.

P8L16: "less affected by blow-cloud processes":What does it mean? Isn't it contradicted from "stronger cloud process" in L8

REPLY: We distinguish two main influences on the isotopic signal of surface precipitation (cf. P9L4+5): the initial composition after formation ("cloud signal") and its alteration by below-cloud processes (also called post-condensation processes). If precipitation is 'less affected by below-cloud processes', it carries more of the 'cloud signal' to the surface. If it is 'strongly affected by below-cloud processes', the 'cloud signal' is overwritten by below-cloud processes on the way to the surface. The *influence* of the 'cloud signal' thus depends on the strength of below-cloud processes and not on the *strength* of the 'cloud signal', (referred to as 'cloud processes' by the reviewer).

Comments of referee 2

Answers on specific comments:

Abstract
L11: Does 'equilibration' refer to 'exchange between ambient air and raindrops' or 'temperature-dependent equilibrium fractionation'? The description of the $\Delta\delta\Delta d$ figure in the previous sentence highlights the latter, but I tend to associate equilibration with the former process. L15 also cites equilibration being less when RH is higher – RH would not affect the temperature-dependent equilibrium but would affect the exchange of isotopes between rain and ambient air through rain evaporation and condensation. See Section 2 of Nusbaumer et al (2017) for a good description of the microphysical processes needed to describe isotope ratios in rain and vapor ("Evaluating hydrological processes in the Community Atmosphere Model Version 5 (CAM5) using stable isotope ratios of water", Journal of Advances in Modeling Earth Systems, 9:949-977). Non-equilibrium kinetic fractionation must also be included in this analysis.

REPLY: 'Equilibration' refers to 'exchange between ambient air and raindrops'. By including the 'equilibrium vapour from precipitation samples' ($\delta^2H_{p,eq}$, $d_{p,eq}$) instead of the actual composition of precipitation samples (δ^2H_p,d_p) in Eqs. (5) and (6), we remove the 'equilibrium difference' (cf. P5,L1), which is caused by the 'temperature-dependent isotopic fractionation'. The high relative humidity reduces below-cloud evaporation and the low melting layer reduces time for equilibration and thus affects the 'degree of

equilibration' between rain and vapour on the ground. We agree that the formulation in L15 is somewhat unclear and could be confusing. We therefore rephrased the sentence in the revised manuscript:
"After the frontal passage, the near-surface atmospheric layer is characterised by higher relative humidity, which leads to weaker below-cloud evaporation. Additionally, a lower melting layer after the frontal passage reduces time for exchange between vapour and rain and leads to weaker equilibration."

Section 1

P2, L30: It might help to insert some explanation about Rayleigh distillation along rain back trajectory, which is the starting point for getting to more depleted rain values at higher latitudes.

REPLY: We extended the sentence by the explanation that air at high altitudes (and latitudes) has experienced more rainout and is thus more depleted due to the Rayleigh distillation process. "As heavy isotopes preferentially condense due to their larger mass, air subject to rainout subsequently loses heavy isotopes. The increasing depletion with increasing fraction of rainout along the trajectory of an air parcel can be approximated by the Rayleigh distillation model under most atmospheric conditions (Dansgaard, 1954, Ciais and Jouzel, 1994). Air at higher altitudes and latitudes has on average experienced more cooling and rainout and is thus increasingly depleted of heavy isotopes, reflected in negative δ values."

P2, L31: as long as the air column is unsaturated

REPLY: An exchange of water molecules occurs in both directions under both saturated and unsaturated conditions. At conditions well below saturation, the exchange is strongly one-sided and the condensation of molecules can be practically neglected. At conditions close to saturation however, condensation cannot be neglected, in particular when the isotopic composition of precipitation and vapour are far from their isotopic equilibrium. Thus, the drop and the surrounding vapour will continuously exchange water molecules, also in unsaturated conditions. We clarified this by adding the following sentence to the end of the paragraph:
"It is relevant when the air column is at or near saturation."

P3, para1: Some introduction about kinetic fractionation would be appropriate here.

REPLY: Also in response to comments by Reviewer #1 we include now a more detailed introduction of kinetic fractionation by adding:

"In unsaturated conditions, a net transfer of water molecules from the drops to the surrounding air does occur. In addition to the equilibrium fractionation that happens during this transfer, the slower diffusion of the heavy molecules $^{1}H^{2}H^{16}O$ and $^{1}H_{2}^{18}O$ causes additional non-equilibrium or kinetic fractionation. Thereby, lower relative humidity leads to more intense non-equilibrium fractionation. The second-order parameter d-excess ($d = \delta^{2}H - 8 \cdot \delta^{18}O$) is sensitive to such non-equilibrium conditions, where $^{2}H^{1}H^{16}O$ reaches isotopic equilibrium faster than $^{1}H_{2}^{18}O$. The d-excess quantifies the difference in $^{2}H^{1}H^{16}O$ and $^{1}H_{2}^{18}O$ from their ratio expected during equilibrium conditions as a measure of non-equilibrium (Dansgaard, 1964; Stewart, 1975). Evaporation of rain in unsaturated conditions causes a decrease of d-excess in rain and consequently an increase of d-excess in the surrounding air. Further parameters critically influence this process, such as the drop size distribution (Managave et al., 2016), below-cloud relative humidity (Lee and Fung, 2008), the height of the melting layer, the height of the cloud base (Wang et al., 2016), and vertical wind velocity. Thus, isotopes reflect the conditions acting on rain below the cloud, but in convoluted ways that often render interpretation cumbersome."

Section 2

P4, L2: How much of the data was discarded for both measurements and calibrations? This is typically done to ensure no memory effects on the final values.

REPLY: We discarded the first 10 minutes of ambient air measurements after each calibration. From the calibration, we discarded the first 5 minutes and the last 30 seconds. Thanks to your comment, we also discovered that the duration of the calibration was in fact 15 min. The text was adjusted accordingly and a sentence to add the discarded amount of data was added:

"The first 5 minutes and last 30 seconds of the calibration, as well as the 10 min ambient air measurements after each calibration were discarded to avoid the influence of memory effect on calibration and the final isotope data."

P4, L9: Was any oil added to the funnel to prevent evaporation during collection? Did the authors check for potential sample evaporation over 30 minutes, especially if the air was unsaturated? This could especially complicate the interpretation of d-excess values.

REPLY: We did not add oil to the funnel (or into the vial) or check for potential sample evaporation. We tried to reduce evaporation effects by keeping collection intervals short and by choosing PTFE as material for the funnel, which has reduced adhesion of droplets on its surface compared to other materials.

P5, L4: This is also complicated by needing to know both temperature of vapor and rain.

REPLY: We apologize but we did not understand this comment.

P5, L15: Is ambient temperature accurately reflecting raindrop temperature? Wouldn't it be better to look at "equilibrium precipitation from vapor", since ambient temperature is more likely to represent the ambient vapor? I would suggest repeating the analysis using this direction (or at least check to see if it makes a difference). Especially given the authors' explanation for non-linearity in temperature control of isotope ratios.

REPLY: Since the net mass flux in an unsaturated environment is from the droplet to the ambient air, we consider it more intuitive to define the equilibrium vapour from precipitation. We emphasize this now when defining this quantity in the manuscript. Ambient temperature is higher than raindrop temperature due to (i) temperature lag of falling precipitation, which carry a bit of the colder temperature aloft and (ii) evaporative cooling. While the temperature difference due to (i) is small (< 0.2°C for d=2mm and lower for smaller drop diameters; Graf 2018; Fig 3,2b between 1000 and 2200m), it is larger due to (ii), and reaches 2.5°C for an ambient relative humidity of 75%. Looking at the 'equilibrium vapour from precipitation' using ambient temperature introduces an error of approximately 2.5‰ for $\Delta\delta$ and 1‰ for Δd when assuming a change of the equilibrium difference between vapour and liquid of 1‰/°C and 0.4‰/°C, respectively (cf. Table 1 of the manuscript). Interestingly, the temperature difference between rain and vapour depends mainly on the relative humidity and not on the drop diameter (cf. Fig 3,2b below 1000m in Graf, 2018). The rain temperature can thus be approximated from ambient air temperature and relative humidity measurements instead of measuring it directly.

P5, L24: Do you get the same results using δ 18O observations instead for eqn (5)?

REPLY: δ^2H is more strongly influenced by kinetic fractionation than $\delta^{18}O$. The results, in particular $\Delta d/\Delta\delta$, are thus numerically different, while the conclusions remain unchanged.

Section 3

P7, L19: I assume the correlations reported here are significant with p values < 0.05? Could add 'significant' to line 19. Correlation with h has been seen by others (Crawford et al 2016), especially in unsaturated semi-arid environments. Correlation with rain intensity/amount is traditionally assigned to the classic 'isotopic amount effect'. Some discussion of these would be appropriate here.

REPLY: Yes, the reported correlations are all significant with p values < 0.05; "significant" was added as suggested. We have split this section in the revised manuscript and in this revised context the discussion of other literature and of the amount effect does not fit well into the discussion.

P7, L24: Consider: is the 'surrounding vapor' simply the vapor coming down with the rain in a downdraft? In which case I would expect them to be closely correlated. Can you distinguish this from non-downdraft/near-surface surface vapor being influenced by rain?

REPLY: With ‘surrounding vapour’, we denote the local near-surface vapour, which is subsequently altered in terms of isotopic composition by the air falling through it. Downdrafts may contribute to the ambient vapour in convective conditions. The frontal passage considered here was however of dominantly stratiform nature, as confirmed by the low variability of the surface vapour isotope composition. We mention the mainly stratiform nature of the frontal precipitation event in the revised manuscript.

Section 4

Fig 3 and P7, L30: how do you distinguish ‘rain samples in equilibrium with vapor’ – is this the zero line? I don’t see samples at 17 UTC near the zero line for Δδ or for Δd at 21 UTC (looks more like 22 UTC). There are several periods where the uncertainty of Δd overlaps the zero line.

REPLY: With ‘rain samples in equilibrium with vapour’ we describe samples near the zero line, ideally with an overlap of the uncertainty with the zero line. For Δd, this is the case for several samples, in particular during the post-frontal phase. We gave the samples around 19 UTC and the four samples just before 21 UTC as examples, since they match the zero line almost perfectly. The uncertainty of Δδ is very small and thus only few overlaps occur. We chose 17 UTC as an example, because then Δδ changes from positive to negative. A hypothetical continuous time series would intersect the zero line and be in equilibrium with vapour, although this is not the case for a particular sample. Choosing the time 17 UTC as example is thus somewhat confusing and was changed to 15 UTC. We adapted the text slightly to clarify this:
“Some rain samples are in equilibrium with vapour for δ^2H (Δδ≈0‰; e.g. at 15 UTC), for *d* (Δd≈0‰; at about 19 and before 21 UTC) or for both (Δδ and Δd≈0‰; at 10 UTC).”

P7, L32-33: More negative values of Δδ are seen before the frontal passage, with Δd trending towards zero. Some explanation of what is going on here? Also, if there is conservation of the depleted isotopic signature from the cloud, I think this should also be reflected in Δd being zero. Any partial/incomplete tendency towards equilibration should be seen in both signatures from the way equations (5) and (6) are set up. If the argument is for ‘conservation’, i.e. vapor reflecting the original rain signature in equilibrium (possibly because it is associated with a downdraft associated with the frontal passage), this should be captured in both Δδ and Δd.

REPLY: We assume that this comment refers to the samples in the two hours before the frontal passage (between 17 and 19 UTC), which are already negative for Δδ but not yet close to zero for Δd.

Considering first the second part of the comment, we agree that the influence of the ‘cloud signal’ and its (partial) conservation is theoretically reflected in both Δδ and Δd. However, the difference of the isotopic composition of precipitation after formation (‘cloud signal’) and at the surface is much larger for Δδ than for Δd. δ_v at cloud-level (and thus the initial $\delta_{p,eq}$) is very depleted compared to vapour at the surface. Thus, a large change in δ_p has to be performed by below-cloud processes in order for rain to arrive at the surface in or close to equilibrium with near-surface vapour. A low melting layer, intense rain or a high below-cloud humidity limit the strength of below-cloud processes and conserves some of the negative Δδ. The situation for Δd is different: The difference between ‘cloud signal’ and $d_{p,eq}$ at the surface is smaller, mainly due to the absence of a strong vertical gradient of d_v, and due to the reasons mentioned in P9,L11-14. It is more easily overcome, even if the time for equilibration is limited. The ‘cloud signal’ is thus only conserved in cases where equilibration is strongly limited. Consider also, that the ‘cloud signal’ of d-excess is usually close to, but not necessarily 0‰. A d-excess, which is close to 0‰ or even positive is not necessarily the result of incomplete equilibration and conservation of cloud signal. It is rather an evidence that evaporation, which strongly decreases Δd, was weak. In the revised version of the manuscript, this is now illustrated clearly in simulations with an idealised model of below-cloud processes.

Regarding the first part of the reviewer’s comment, a decrease in Δδ is not necessarily linked to an increase of Δd because below-cloud processes have different pathways in the ΔδΔd-space. (i) a change in the degree of equilibration can lead to changes in Δδ without having an effect on Δd, if Δd is already fully equilibrated (at the surface or aloft, before Δd is decreased by evaporation) and (ii) a change in the intensity of evaporation will lead to a large change in Δd, whereas Δδ is affected less strongly. We explain the signal of the samples between 17 and 19 UTC as follows: Δd is low because it reflects the low relative humidity before the frontal passage. The increase in relative humidity should cause an increase of Δd, which is

however partially counteracted by the increasing conservation of a negative Δd from aloft. The decrease of Δδ confirms this increasing conservation of the signal from aloft. It can be explained by the increasing precipitation intensity in this phase, which reduces equilibration. The strong increase in Δd during the frontal passage is then mainly caused by reduced evaporation, which also affects Δδ, but less strongly.

Fig 4, P8 L6-7: Some discussion of how non-equilibrium kinetic effects would influence the evolution of the Δδ and Δd signals would be appropriate here. Why would the early pre-frontal samples be expected to be around the (0,0) point? Falling through an unsaturated atmosphere at 75-85% humidity, I would expect to see more evaporation and kinetic effects. Fig 4a is easier to interpret, the various transitions during the progression of the rain event are harder to read in Fig 4b.

REPLY: Kinetic effects during evaporation of rain act in the ΔδΔd-space as a vector towards the bottom right side of the diagram, since it decreases Δd and increases Δδ. The slope of this vector is around –1.3 Δd/Δδ (see comment #3 of referee 1, Figure A) with weak dependencies on remaining fraction, temperature and isotopic composition of rain. Non-equilibrium effects are characterised by a vector that points towards (0,0). The trajectory of rain in the ΔδΔd-space depends on the relative contribution of these two vectors. In low relative humidity conditions, the evaporation vector dominates the overall trajectory (or tendency of the interconnected points in Fig. C with decreasing rain rate), which therefore points towards the bottom right of the diagram. During high relative humidity conditions, the evaporation vector is short and equilibration dominates the overall trajectory, which therefore points towards the origin. The explanation of non-equilibrium effects on the evolution of Δδ and Δd signals has been added in the revised manuscript, due to the inclusion of the idealised simulations with a below-cloud interaction model.

Considering the question about the early pre-frontal samples: Assuming that the said rain samples start with Δd≈0 and fall through an atmosphere with a relative humidity of 80-85% (the samples with RH=75% exhibit a clearly negative Δd), we would indeed expect them to be at more negative Δd. While we cannot provide a final explanation, possible reasons are, e.g., a positive initial Δd, which first has to be compensated by evaporation, before negative Δd occurs, or that the near-surface humidity is not representative of the air column, which may me more saturated in this period of the event.

Lastly, we agree that the various transitions are not perfectly obvious in Fig. 4b, but less obscure than when we connect the dots or display sample numbers. The longer-term progression and transitions should however stand out sufficiently in Fig. 4b to allow following the discussion.

Section 5

P9, para 2: Here the discussion of Δδ and Δd is in terms of precipitation, while previously it was defined as the difference in precipitation-equilibrated and surface vapors.

REPLY: The use of Δδ and Δd is not necessarily confined to precipitation signals at the surface. It makes sense to apply it to precipitation aloft when studying its evolution in the ΔδΔd-space during the sedimentation from the cloud to the ground. To keep a constant frame of reference with height, we always use surface values of δ^2H_v and d_v, while values from aloft can be used for $\delta^2H_{p,eq}$ and $d_{p,eq}$. Thus, we can use Δδ and Δd to describe the isotopic composition of precipitation and its evolution during the sedimentation from the cloud to the ground, which can help us to understand the processes that determine the location of precipitation at the surface in the ΔδΔd-space. This is now explained in the revised version of the manuscript. More detailed explanations of the evolution of precipitation in the ΔδΔd-space are illustrated in Fig. B (see below), which is also included in the revised manuscript as part of the idealised model simulations. Furthermore, we added clarifying subscripts to eqs. (5) and (6) to denote that the vapour isotope composition is always taken from the surface, while the equilibrium precipitation composition can be taken for any level of the column to describe a temporal evolution:

$\Delta\delta = \delta^2H_{p,eq} - \delta^2H_v^{sfc}$ and
$\Delta d = d_{p,eq} - d_v^{sfc}$.

P9, L11: Assuming the precipitation is in equilibrium with the vapor it formed from in the cloud (through temperature equilibration), I would expect the Δd of rain versus 'vapor-where-the-rain-formed-in-the-cloud' to be small, but it could still be vastly different from the Δd at the surface.

REPLY: See also first part of the answer to comment P7 and P9. Intuitively, one would indeed assume, that the difference between $d_{p,eq}$ and d_v (at any given height, i.e. a local value of Δd) is small where precipitation is formed. This is however not the case due to the following reasons:

Kinetic effects during formation through the Wegener-Bergeron-Findeisen process in mixed-phase clouds involves supersaturation and thus kinetic effects, which can increase $d_{p,eq}$ by more than 10‰. Also, the d-excess change during equilibrium fractionation is very different for the vapour-solid than for the vapour-liquid transition. Thus, $d_{p,eq}$ of rain is lower by 13.4‰ compared to $d_{p,eq}$ of snow for $\delta^2H_l = -120$‰ and d_l=0‰ at 0°C. (see Table 1). When changing the phase across the melting layer, $d_{p,eq}$ of precipitation thus decreases. The increase due to kinetic processes and the decrease due to the difference between the vapour-solid and vapour-liquid transition partly compensate each other. In the case presented in Fig. B, the difference between $d_{p,eq}$ and d_v (the local Δd) after formation and at the 0°C-isotherm is negative (–7.5‰ and –5‰; note that the 'column Δd' is shown. The 'local Δd' is however almost equal, since $d_v \approx d_v^{sfc}$). Under different conditions (e.g., lower formation temperatures, which enhance the kinetic effects), the difference might as well be positive.

The locally calculated Δd in the cloud and the Δd at the ground, as defined in the manuscript, can be vastly different due to three reasons: (i) If the local Δd in the cloud is very different from 0‰ and equilibration will reduce its absolute values, (ii) if evaporation strongly decreases $d_{p,eq}$, and (iii) if the vertical gradient of d_v is large. This is underlined by the case presented in Fig. B: The local Δd in the cloud is not small, but the difference between the local Δd in the cloud and on the ground is small (at least for D=0.5 mm and 1 mm).

In addition to the inclusion of the idealised model simulations, we added the vapour-solid transition at 0°C to Table 1 and deleted part of the sentence at P9,L14, because this effect is already included in the definition of $d_{p,eq}$: "and by a decrease due to the non-linearity of the δ-scale (Dütsch et al., 2017)".

P9, L15: Raindrops will also get more enriched during evaporation into an unsaturated atmosphere, because the lighter isotopes are preferentially evaporated, which will make the ambient vapor more depleted.

REPLY: We did not discuss the effect of below-cloud processes on ambient vapour, which is of course also something to consider. However, on short enough time-scales (a hydrometeor falling from the cloud to the ground), the effect on vapour can be neglected, since the amount of vapour in an air parcel exceeds the amount of liquid or solid by far, especially for the rain rates we measured (for the calculation see Section 4.2 in Graf, 2018). The effect on vapour would only appear over a longer time period. In the event we present here, a part of the gradual depletion of vapour after ~16 UTC could be caused by interaction with falling precipitation or downward motion of the air, which introduces depleted moisture. This discussion has been included in the description of the time evolution of the vapour isotope measurements of the front.

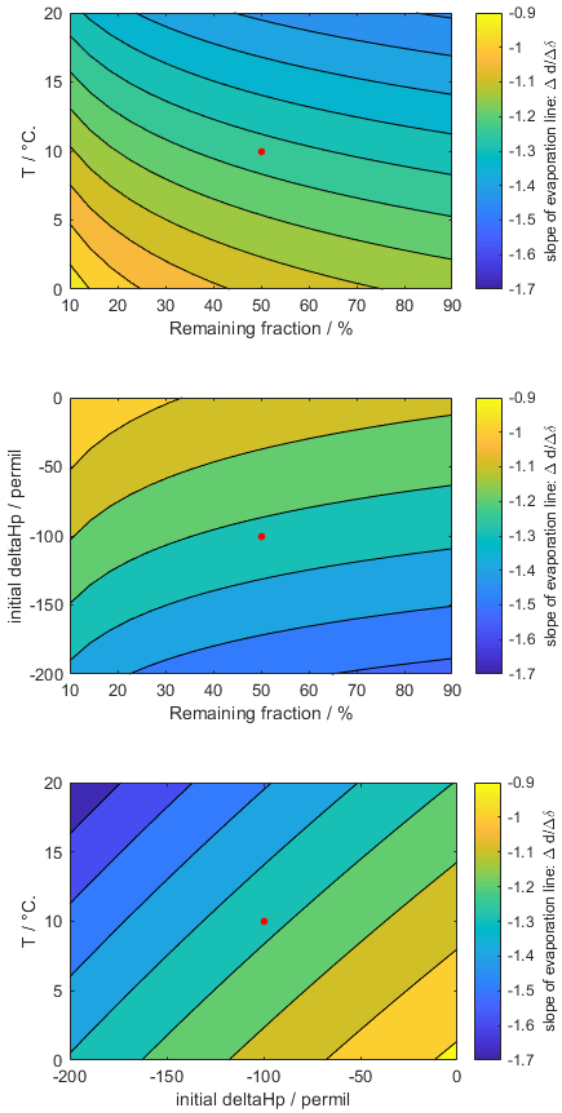

Figure A: Slope of evaporation line, $\Delta d / \Delta \delta$, as a function of (top) temperature and remaining fraction, (middle) initial $\delta^2 H_p$ and remaining fraction, and (bottom) temperature and initial $\delta^2 H_p$.

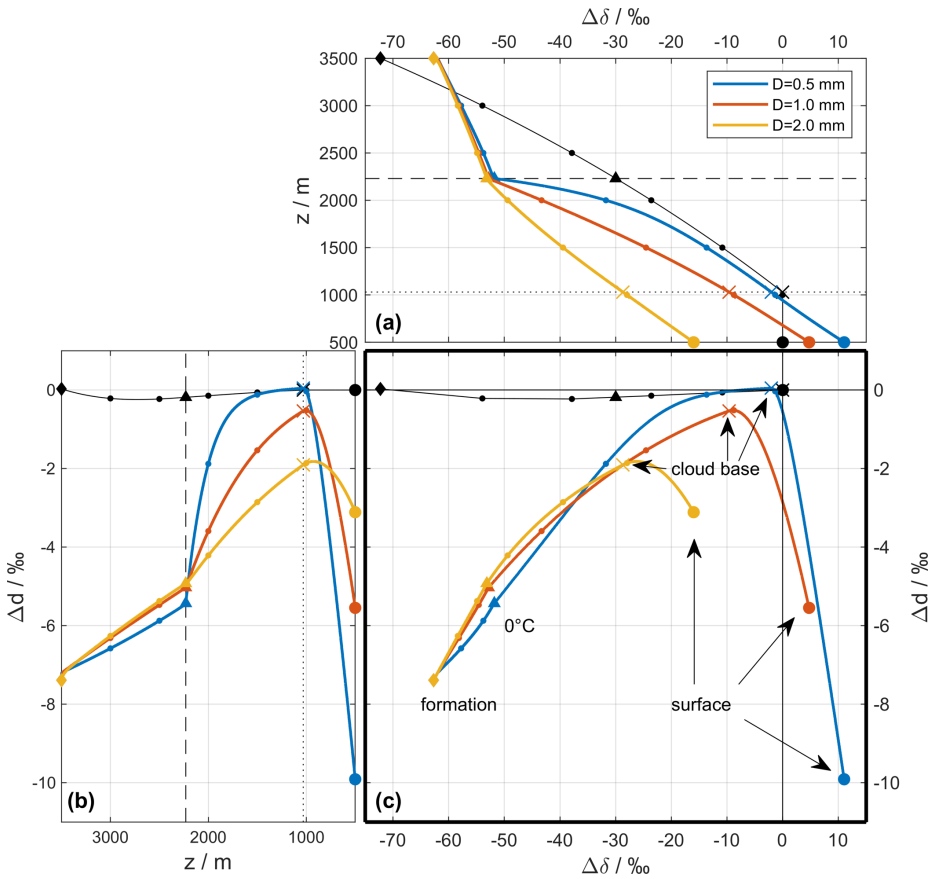

Figure B: Simulated evolution of the isotope composition of a droplet using the idealised below-cloud process model. (a) Δδ vs. droplet elevation, (b) Δd vs. droplet elevation, (c) Δδ-Δd diagram for the droplets. Coloured lines denote different droplet diameters, black line denotes background vapour composition.

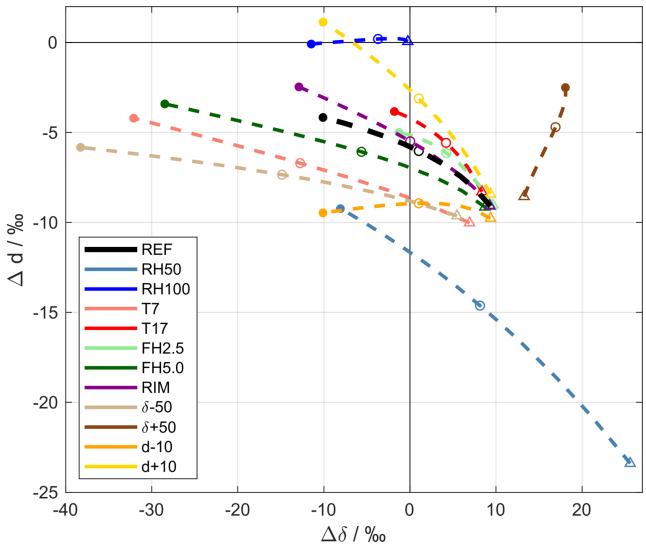

Figure C: Sensitivity of Δδ and Δd for the surface vapour and equilibrium vapour for precipitation to variations of the idealised model setup. For details see the revised manuscript.

Geophysical Bjerknes

A new interpretative framework for below-cloud effects on stable water isotopes in vapour and rain

Pascal Graf[1], Heini Wernli[1], Harald Sodemann[1,2,3], Stephan Pfahl[1,2], and Harald Sodemann[1,3,4]

[1]Institute for Atmospheric and Climate Science, ETH Zurich, Zurich, Switzerland
[2]Institute of Meteorology, Freie Universität Berlin, Berlin, Germany
[3]Geophysical Institute, University of Bergen, Bergen, Norway
[4]Bjerknes Centre for Climate Research, Bergen, Norway

Correspondence: Harald Sodemann (harald.sodemann@uib.no)

Abstract. Raindrops interact with water vapour in ambient air while sedimenting from the cloud base to the ground. They constantly exchange water molecules with the environment and, in sub-saturated air, they evaporate partially or entirely. The latter of these below-cloud processes is important for predicting the resulting surface rainfall amount and it influences the boundary layer profiles of temperature and moisture through to evaporative latent cooling and humidity changes. However, despite its importance, it is very difficult to quantify this process from observations. Stable water isotopes provide such information, as they are influenced by both rain evaporation and equilibration. This study elucidates this option by introducing a novel interpretation interpretative framework for stable water isotope measurements performed simultaneously at high temporal resolution in both near-surface vapour and rain. We refer to this viewing device as the $\Delta\delta\Delta d$-diagram, which shows the isotopic composition (δ^2H, d-excess) of equilibrium vapour from precipitation samples relative to the ambient vapour. It is shown that this diagram facilitates the diagnosis of below-cloud processes and their effects on the isotopic composition of vapour and rain since equilibration and evaporation lead to different pathways in the two-dimensional phase space of the $\Delta\delta\Delta$ d-diagram. For d-diagram, as investigated with a series of sensitivity experiments with an idealized below-cloud interaction model. The analysis of isotope measurements for a specific cold front in Central Europe, the analysis Europe shows that below-cloud processes lead to distinct and temporally variable imprints on the isotope signal in surface rain. The influence of evaporation on this signal is particularly strong during periods with a weak precipitation rate. After the frontal passage, the near-surface atmospheric layer is characterised by higher relative humidity and humidity, which leads to weaker below-cloud evaporation. Additionally, a lower melting layer, leading layer after the frontal passage reduces time for exchange between vapour and rain and leads to weaker below-cloud evaporation and equilibration. Measurements from four cold frontal events reveal a surprisingly similar slope of $\frac{\Delta d}{\Delta \delta} = -0.30$ in the phase space, indicating a potentially characteristic signature of below-cloud processes for this type of rain events. event.

1 Introduction

Processes acting during the short travel of rain through the atmosphere from the cloud base to the surface ~~has a,~~ have a maybe ~~surprisingly,~~ surprisingly large relevance for several atmospheric phenomena. The two-phase system of rain and vapour is in constant molecular exchange. In addition, in unsaturated conditions, rain partially evaporates, leading to latent cooling of the air, and moistening of the boundary layer. Surface rainfall totals may be substantially ~~lower~~ reduced in cases of strong evaporation (Aemisegger et al., 2015), and in the case of convection in the Sahel, large evaporation-driven cold pools can trigger extensive dust storms known as haboobs (Roberts and Knippertz, 2012). In mid-latitudes, cold pool formation influences low-level moisture convergence and thereby the progression and organisation of convective systems (Bennett et al., 2007).

Measurements of these so-called below-cloud processes (Aemisegger et al., 2015) are challenging. ~~Common radiosondes~~ Radiosonde profiles provide instantaneous snapshots of a vertical profile of humidity and temperature, but do not capture precipitation rates, and are expensive when deployed at high frequency. ~~Radar data on the other hand~~ Precipitation radar can continuously provide vertically resolved ~~drop spectra,~~ spectra of rain drops, but ~~do neither~~ does not provide information about relative humidity ~~nor~~ and temperature, which are necessary to reasonably quantify precipitation evaporation (Xie et al., 2016). Other remote-sensing systems, such as Raman water vapour lidar (Cooney, 1970), Fourier transform infrared radiometers (Schneider and Hase, 2009) and passive microwave radiometers (Solheim et al., 1998) provide vertical profiles of humidity, but are strongly attenuated during precipitation.

As a consequence of the lack of sufficient observations, ~~models use poorly constrained~~ model parameters ~~to~~ that represent the interaction of falling raindrops with the air column below the cloud ~~base.~~ base are poorly constrained. Errors in the representation of this process ~~diminishes~~ diminish the model forecast quality due to its impact on the rainfall amount and the dynamics of ~~a~~ weather ~~system.~~ systems. This issue becomes even more relevant as common weather prediction ~~models~~ models, such as COSMO (Steppeler et al., 2003), WRF (Skamarock et al., 2008), or AROME (Seity et al., 2010) progress to resolution beyond the grey ~~zone, where~~ zone. At horizontal resolutions below about 10 km precipitation is commonly implemented as a prognostic ~~variable ,~~ variable, and convective updrafts, downdrafts and the formation of cold pools are partly resolved at the grid scale. These modelling challenges provide an additional motivation to ~~deepen our understanding of~~ better understand below-cloud processes.

In this context, stable isotopes of water vapour and rain are useful to investigate below-cloud processes. Stable water isotopes are natural, passive tracers that ~~integrate over~~ reflect the phase-change history of water. The stable isotope composition is quantified using isotope ratios, defined as the concentration of the rare (heavy $^{2}\mathrm{H}^{1}\mathrm{H}^{16}\mathrm{O}$ or $^{1}\mathrm{H}_{2}^{18}\mathrm{O}$) over the abundant (light $^{1}\mathrm{H}_{2}^{16}\mathrm{O}$) isotope, e.g.:

$$^{2}R = \frac{[^{2}\mathrm{H}^{1}\mathrm{H}^{16}\mathrm{O}]}{[^{1}\mathrm{H}_{2}^{16}\mathrm{O}]} \,. \tag{1}$$

Most studies use the more intuitive δ notation (Dansgaard, 1964; Galewsky et al., 2016), which expresses the heavy isotope composition of a reservoir in terms of relative deviation of R from an internationally accepted standard:

$$\delta = \frac{R_{\mathrm{sample}} - R_{\mathrm{standard}}}{R_{\mathrm{standard}}} \cdot 1000‰ \,. \tag{2}$$

A δ value is defined for both heavy over light isotope concentrations (δ^2H and δ^{18}O) and generally indicated in per mil (‰) relative to Vienna Standard Mean Ocean Water (VSMOW2; IAEA, 2009). As heavy isotopes preferentially condense due to their larger mass, ~~vapour in higher levels~~ air subject to rainout subsequently loses heavy isotopes. The increasing depletion with increasing rainout along the trajectory of an air parcel can be approximated by the ~~atmosphere are~~ Rayleigh distillation model (Dansgaard, 1954; Ciais and Jouzel, 1994). Air at higher altitudes and latitudes has on average experienced more cooling and rainout and is thus increasingly depleted of heavy isotopes, reflected in more negative ~~δ values.~~ δ-values. As precipitation forms from this vapour depleted in heavy isotopes, temperature-dependent fractionation will lead to a relative enrichment of heavy isotopes in the ~~precipitation.~~ hydrometeors. Typically, though, precipitation δ values will still be depleted relative to the standard ocean water VSMOV2, as expressed in negative ~~delta~~ δ values. As ~~precipitation falls~~ rain drops fall through the air column, ~~the drop and the surrounding vapour will~~ they continuously exchange water ~~molecules.~~ molecules with the surrounding vapour. This exchange is particularly relevant if the air column is at or near saturation. Thermodynamics will direct this exchange towards isotopic equilibrium according to ambient temperature. This process is termed *equilibration* and only occurs when the precipitation is liquid.

In unsaturated conditions, a net transfer of water molecules from the drops to the surrounding air ~~does occur.~~ occurs. In addition to the equilibrium fractionation that happens during this transfer, the slower diffusion of the heavy molecules ^{2}H^{1}H^{16}O and ^{1}H$_2^{18}$O causes non-equilibrium or kinetic fractionation. Thereby, lower relative humidity leads to more intense non-equilibrium fractionation. The second-order parameter d-excess ($d = \delta^2\mathrm{H} - 8 \cdot \delta^{18}\mathrm{O}$) is sensitive to such non-equilibrium conditions, ~~where~~ since ^{2}H^{1}H^{16}O reaches isotopic equilibrium faster than ~~^{1}H$_2^{18}$O.~~ ^{1}H$_2^{18}$O (Dansgaard, 1964). The d-excess quantifies the difference in ^{2}H^{1}H^{16}O and ^{1}H$_2^{18}$O from their ratio expected during equilibrium conditions as a measure of non-equilibrium ~~.~~ (Stewart, 1975). Evaporation of rain in unsaturated conditions causes a decrease of d-excess in rain and consequently an increase of d-excess in the surrounding air. Further parameters critically influence this process, such as the drop size distribution (Managave et al., 2016), below-cloud relative humidity (Lee and Fung, 2008), the height of the melting layer, the height of the cloud base (Wang et al., 2016), and vertical wind velocity. Thus, isotopes reflect the conditions ~~acting on~~ that rain drops experience below the cloud, but in a convoluted ~~ways~~ way that often ~~render~~ renders interpretation cumbersome. If stable isotope are to be used for constraining below-cloud processes, different factors need to be disentangled.

Previous studies often investigated only ~~one~~ the condensed part of the two-phase system (e.g., Miyake et al., 1968; Celle-Jeanton et al., 2004; Barras and Simmonds, 2009; Risi et al., 2010; Muller et al., 2015; Managave et al., 2016). ~~They studied~~ These studies sampled rain in high temporal resolution and ~~came up with partially~~ gave sometimes contrasting explanations for the observed short-term isotopic variations. For example, Coplen et al. (2008) and Yoshimura et al. (2010) investigated an atmospheric river event in California and disagreed on whether below-cloud processes or changes in the formation height caused the variations they observed. ~~showed for a mid-latitude rain event that joint observations in vapour and rain reveal the influence of below-cloud processes more clearly and contain information on the structure of the precipitation system.~~ Since vapour and rain are in ~~a~~ continuous exchange, measuring one without the other makes meaningful interpretation difficult. This is especially the case in situations dominated by advection, for example cold-frontal rain. There, the isotopic evolution of rain is a combined signal of a changing air mass and ~~cloud signal,~~ in-cloud processes, below-cloud equilibration with progressively

depleted vapour as the front progresses, and rain evaporation (Dütsch et al., 2016). Simultaneous observations of vapour and precipitation are necessary to distinguish these processes and quantify below-cloud processes. Aemisegger et al. (2015) showed for a mid-latitude rain event that combined observations of stable isotopes in vapour and rain more clearly reveal the influence of below-cloud processes and the structure of the precipitation system.

Thus, joint observations of the stable isotope composition of vapour and precipitation at ground level are ~~valuable, as they contain~~ valuable recorders of the convoluted influence of ~~different~~ several factors and processes. However, ~~for the same reason,~~ extracting the ~~main driving~~ contribution of individual factors is ~~a difficult task.~~ challenging. Here we ~~introduce~~ propose a new set of measures to ~~single out~~ quantify the influences of equilibration and evaporation on the isotope composition of near-surface vapour and rainfall. ~~Using high-resolution joint isotope data from cold fronts in Central Europe, we introduce~~ To this end, a new ~~viewing and interpretation device,~~ interpretative framework is introduced, which allows us to determine the leading below-cloud processes during a precipitation event. This framework is used here to interpret both high-resolution isotope measurements from cold fronts in Central Europe and results from idealized simulations with a below-cloud interaction model. Section 2 provides information about the measurements and the below-cloud model. The stable water isotope measurements during a cold frontal passage are presented in Section 3. Section 4 introduces the new interpretative framework with an idealized model, before the observations are discussed in the new interpretative framework in Section 5. Finally, we provide our main conclusions in Section 6.

2 Data and Methods

2.1 Isotope measurements

Stable water isotopes in ambient water vapour were measured on a tower building at the Institute for Atmospheric and Climate Science of ETH Zurich (47.38°N, 8.55°E; 510 m a.s.l) between 9 October and 27 November 2015 with a cavity ring down spectrometer (L1115-i, Picarro Inc, USA). Ambient air was directed to the analyser through a 10 m PFA tubing heated to 70°C that was flushed by a bypass pump (HN022AN.18, KNF Neuberger, Germany) with a flow rate of 9 $l\,\mathrm{min}^{-1}$ (Aemisegger et al., 2012; Aemisegger, 2013). The isotopic analyser was calibrated twice a day at ambient humidity levels using a commercial setup (Standards Delivery Module A0101 and Vaporizer V1102-i, Picarro Inc. USA). Two laboratory standards bracketing the composition of typical ambient values in ambient vapour (Standard 1: $\delta^2\mathrm{H} = -75‰$, $\delta^{18}\mathrm{O} = -10‰$; Standard 2: $\delta^2\mathrm{H} = -247‰$, $\delta^{18}\mathrm{O} = -43‰$) were provided to the analyser for ~~15 min~~ 10 min each. The first 5 min and last 30 s of the calibration, as well as the 10 min ambient air measurements after each calibration were discarded to avoid the influence of memory effect on calibration and the final isotope data. Raw measurements were corrected with an average calibration function from all calibration runs of the measurement period. Frequent gaps in the calibration make this time-independent calibration function more robust compared to the usual linear interpolation between subsequent calibration runs. The thereby neglected shorter-term drift leads to an increased uncertainty of the calibrated measurements. The 5 s measurements of the instrument were transformed to 10 min average values, which have an average uncertainty after calibration of 1.23‰ for $\delta^2\mathrm{H}$, 0.42‰ for $\delta^{18}\mathrm{O}$, and 3.6‰ for d-excess. For more details about the vapour isotope ~~measurements,~~ measurements see Graf (2017).

At the same location, rain was manually sampled during selected events with a simple rainfall collector. The collector consists of a PTFE funnel of 15 cm diameter, which points into a 20 ml glass vial. Each sample was collected in a separate vial, which was immediately closed after retrieval from the sampler to avoid evaporation after sampling. A default sampling interval of 10 min was applied, which was shortened to 5 min during intense rain, or prolonged up to ~~30 minutes~~ 30 min if the sampled amount was not sufficient for analysis. The approximate sample amount was recorded, but not used to determine rain rates. The samples were analysed for their isotopic composition in the laboratory with a cavity ring down spectrometer (L2130-i, Picarro Inc., USA) operating for liquid sample analysis (Graf, 2017). The average uncertainty of the calibrated liquid samples is 1.25‰ for δ^2H, 0.24‰ for δ^{18}O and 1.43‰ for d-excess. In this study, 86 continuous rainfall samples collected during a cold frontal passage on 20 November 2015 are presented.

Also measured at the same location were temperature, humidity, wind speed and direction, and precipitation amount and intensity. These parameters were obtained at a 10 min interval from different meteorological sensors (Thygan VTP37 and wind gauge WN37, meteolabor AG; Tipping bucket rain gauge 7051.1000, Theodor Friedrichs & Co.) on the rooftop with measurement distance of less than 5 m to the ambient air inlet of the isotopic analyser.

2.2 Equilibrium vapour from precipitation

~~Rain falling from the clouds~~ Falling rain and the vapour in the atmospheric column below cloud base compose a two-phase system. The ~~liquid precipitation and the surrounding water vapour~~ constant exchange of water molecules ~~during fall, leading~~ makes the system evolve towards an equilibrium in the isotopic composition of both phases. In isotopic equilibrium, there is no net exchange of ~~molecules~~ isotopologues between the ~~phases, i.e., the exchange in both directions is equal for all isotopic species.~~ phases. Temperature-dependent isotopic fractionation between light and heavy isotopes however ~~gives rise to~~ creates different isotopic compositions of the liquid and vapour phases in equilibrium:

$$R_l = \alpha_{v\to l}\, R_v\,, \tag{3}$$

which can be equivalently expressed in δ-notation as

$$\frac{\delta_l}{1000} + 1 = \alpha_{v\to l}\left(\frac{\delta_v}{1000} + 1\right). \tag{4}$$

Here, subscripts l and v denote the liquid and vapour phase, respectively, and $\alpha_{v\to l}$ is the temperature-dependent fractionation factor of the vapour to liquid phase transition. At 20°C, $\alpha_{v\to l}$ is 1.0850 for $^2\mathrm{H}^1\mathrm{H}^{16}\mathrm{O}/^1\mathrm{H}_2^{16}\mathrm{O}$ and 1.0098 for $^1\mathrm{H}_2^{18}\mathrm{O}/^1\mathrm{H}_2^{16}\mathrm{O}$ (Majoube, 1971).

We denote the difference ~~between the two phases~~ due to fractionation between two phases in equilibrium as *equilibrium difference* ~~$\Delta_{l=v}$. The equilibrium difference makes it cumbersome to judge whether two phases are in equilibrium from comparing their δ-values only. The dependence of the equilibrium difference on temperature and isotopic composition further complicates matters, in particular for the interpretation of the d-excess .~~

~~Consider, for example, the~~ $\Delta_{l-v} = \delta_l - \delta_v$. Consider, for example, the equilibrium difference for a vapour-liquid system, where the liquid has a composition of ~~0‰~~ $\delta_l = 0‰$ for both δ^2H and δ^{18}O (A in Table **??**). Δ_{l-v} for δ^2H ~~at 20°C~~ is 78.4‰ at 20°C and 101.0‰ at 0°C. Thus, equilibrium fractionation for cold temperatures is stronger and leads to a larger equilibrium difference of δ^2H and δ^{18}O. In addition, these differences are smaller if the liquid is more depleted in heavy isotopes. For a liquid with $\delta^2\mathrm{H} = -120‰$, Δ_{l-v} becomes 69.0‰ at 20°C, and 88.9‰ at 0°C (B in Table **??**). The increase in fractionation strength with decreasing temperature is stronger for δ^2H than for δ^{18}O, which leads to a more positive equilibrium difference for d towards colder temperatures. In addition, d of vapour increases and hence the equilibrium difference decreases if the liquid or solid is depleted in heavy isotopes. The dependence of the equilibrium difference on temperature and isotopic composition further complicates matters, in particular for the interpretation of the d-excess (Dütsch et al., 2016).

The problem that the comparison of δ-values in precipitation and ambient vapour is not straightforward can be overcome by comparing the isotopic composition of ambient vapour with the *equilibrium vapour from precipitation* for δ-values and d, termed $\delta_{\mathrm{p,eq}}$ and $d_{\mathrm{p,eq}}$ (Aemisegger et al., 2015). The equilibrium vapour from precipitation is ~~defined~~ calculated as the ~~calculated~~ isotopic composition of ~~a~~ vapour that is in ~~exact~~ equilibrium with ~~precipitation, where~~ rain at ambient air ~~temperature is used in the calculation.~~ temperature. The direction of isotopic exchange then becomes apparent directly from the difference between $\delta_{\mathrm{p,eq}}$ and δ_{v} for the δ-values, and from comparing $d_{\mathrm{p,eq}}$ and d_{v} for the d-excess. This substantially simplifies the interpretation of the state of equilibrium in the liquid-vapour system.

~~Therefore,~~ In principle, it would also be possible to introduce in an analogous way an equilibrium precipitation from vapour. We regard the ~~following~~ concept of equilibrium vapour as more intuitive below cloud base, and use it here.

In the following, we make use of the isotopic composition of the *equilibrium vapour from* ~~*precipitation. Differences*~~ *precipitation* and denote differences between ambient vapour at the surface and precipitation ~~are thereby denoted~~ at any level in the column as:

$$\Delta\delta = \delta^2\mathrm{H}_{\mathrm{p,eq}} - \delta^2\mathrm{H}_{\mathrm{v}} \quad \text{and} \quad \delta^2\mathrm{H}_{\mathrm{v,sfc}} \quad \text{and} \tag{5}$$

$$\Delta d = d_{\mathrm{p,eq}} - d_{\mathrm{v}}. \quad d_{\mathrm{v,sfc}}. \tag{6}$$

A $\Delta\delta$ could also be defined for δ^{18}O, which would require an additional index for $\Delta\delta$ to discriminate between δ^2H and δ^{18}O. Since information about δ^{18}O is already included in ~~d, only δ^2H will be used in this study and~~ d the notation is confined to ~~$\Delta\delta$.~~ $\Delta\delta$ for δ^2H. Note that a value of $\Delta d = 0$ does not indicate the absence of non-equilibrium fractionation. It rather is an indication that the ambient vapour and the equilibrium vapour of the precipitation have experienced a similar degree of kinetic effects.

In the analysis below, we will use $\Delta\delta$ and Δd as ~~introduced here as~~ measures of the deviation of the vapour-precipitation system from equilibrium. For instance, a negative value of $\Delta\delta$ indicates that precipitation is more depleted in δ^2H than ambient vapour, based on the equilibrium difference at ambient temperature discussed above. It will be shown that this results in a

powerful, intuitive interpretative framework (referred to as the $\Delta\delta\Delta d$-diagram) to quantify physical processes between the cloud base and the surface from highly-resolved stable isotope measurements in water vapour and precipitation.

Cold frontal passage on 20 November 2015

We The interpretation of this new diagram will apply the framework outlined above to data be further substantited with results from idealized simulations with a prolonged rainfall period below-cloud interaction model, introduced in northern Switzerland. High-resolution rain and vapour the next subsection.

2.3]

Below-cloud interaction modelIn order to support the interpretation of isotope measurements reveal variations in with our new framework and to quantify the role of different processes, we apply a one-dimensional below-cloud processes during the event.

Meteorological situation

interaction model. The local meteorology of this event was characterised by an extended front over Central Europe, which was model simulates the remnant microphysical and isotopic interactions of a cold front associated falling hydrometeor with a decaying cyclone over the Gulf of Finland. surrounding air, as described in detail in Appendix **??** and Graf (2017). In this section, we lay out its general setup and initialisation.

The nearly zonally oriented front passed Switzerland from model consists of a northerly direction during 20 November 2015, before leading single vertical column that extends from the ground to the genesis of height where a new cyclone over single hydrometeor is introduced. The hydrometeor falls through the Gulf of Genoa on column with its terminal velocity, grows or evaporates, changes its temperature and isotopically equilibrates with the surrounding vapour. Isotope processes are parameterized following day. The rainband associated Stewart (1975) with the cold front extends zonally over a distance separate mass balance equations for all three isotope species (Appendix **??**). Interactions with other hydrometeors (collision and breakup) are neglected. Horizontal and vertical air motion are also neglected, i.e., there is no horizontal advection into or out of about 400 km from the Burgundy (France) across Switzerland to column, and no up- or downdraft. As output, the Lake Constance, with a distinct band model yields vertical profiles of high rain intensity (Fig. **??**a). This intense rainband was embedded in a broader zone with stratiform rain. Near Zurich, the frontal passage led to a decrease of equivalent potential temperature (Θ_e) at 850 hPa hydrometeor size and its isotopic composition. Profiles of more than 12 K temperature, humidity and to a veering the isotopic composition of the wind from southwest surrounding vapour have to be provided to northwest (Fig. **??**b).

Meteorological surface observations

An overview of selected surface measurements between 06 UTC 20 November and 01 UTC 21 November 2015 is shown in Fig. **??**. The local 2-m temperature (T; red line in Fig. **??**a) remained roughly constant during the first part of model as input prior to the event, initialisation with a slight increase before 14 UTC. At 19 UTC, when the surface front arrived at rain. These initial profiles can be specified in two ways: (i) based on measurements or simulations with isotope-enabled atmospheric models (such as COSMOiso, Pfahl et al., 2012), or (ii) calculated from the measurement location, a rapid drop idealised (moist) adiabatic ascent of about 2.5°C in 30 min was recorded. The temperature gradually declined further by about 3.5°C between 20 and 22 UTC and remained constant thereafter, resulting in an overall decrease in 2-m temperature of ∼ 6°C. The local relative humidity (h; blue line in Fig. **??**a) varies between 75 – 85 before air parcel from the frontal passage, and increases surface to values around 85 – 90 thereafter.

The rain associated the top of the model column with this frontal event started in Zurich at 06 UTC 20 November and lasted until 03 UTC 21 November 2015. a Rayleigh fractionation process after reaching saturation (Appendix **??**). The total rain measured profiles are assumed to be unaffected by the falling hydrometeor throughout the simulation. This assumption only holds if a single hydrometeor is considered. When simulating rain gauge on the rooftop was 30.9 mm, whereof 27.5 mm fell events during the part of the event investigated here (07:00 - 23:30 UTC). The intensity varied between 0 which many hydrometeors fall and 3 mm h^{-1}, before increasing briefly to 10 mm h^{-1} as subsequently affect the surface front passed at 19 UTC (Fig. **??**b). Thereafter, surrounding air, the intensity remained relatively high compared assumption becomes invalid over time. A remedy to the period prior this problem would be to reinitialize the frontal passage model regularly with an average updated profiles of 3 mm h^{-1} until approximately 23 UTC, when it decreased to low values for the remainder of surrounding air.

The hydrometeor size is defined as the event. Between 12 and 18 UTC, sustained wind speeds occurred between 5 and 10 m s^{-1}, and therefore the rain intensity was likely underestimated during this period due *equivalent liquid diameter*, which corresponds to the exposed location diameter of the rain gauge. A nearby, less exposed meteorological station at ground level (MeteoSwiss Station Zurich Fluntern, at a distance of 1.3 km) recorded spherical liquid drop with the same mass as the hydrometeor. The model can be initialised with a total amount of rain pre-defined hydrometeor size at the height of 38.3 mm during initialisation. Alternatively, as used in this study, the event.

As an aside, we mention terminal diameter at the decrease of surface can be provided as input. In this case, the hydrometeor size at the height of initialisation is varied iteratively until the 0°C isotherm due to target diameter at the frontal passage. Two balloon soundings, launched from surface is reached. To simulate bulk precipitation, the measurement site in Zurich, indicate model can be run (i) for all bins of a decrease from 2700 m a.s.l. at 16:30 UTC drop size distribution, which are then used to 1500 m a.s.l. at 22:30 UTC (not shown).

Isotopic composition of vapour and rain

~~The 10-minute averaged values were between −35‰ and −14‰ for $\delta^{18}O_v$ (not shown) and between −265‰~~ calculate a mass and ~~−105‰ for δ^2H_v (Fig. **??**c, black line). The vapour isotope measurements exhibit an overall decrease of more than 160‰~~ number-weighted sum or (ii) for ~~δ^2H_v during~~ just one hydrometeor size, which approximates the ~~entire event. A weak decrease~~ drop size distribution with a single diameter. This is represented by the mass weighted mean diameter D_m, which is obtained in ~~δ^2H_v around 08 UTC was followed~~ this study from the rain rate by assuming a ~~steady increase until 14 UTC. δ^2H_v slowly decreased thereafter until approximately 18 UTC when~~ Marshall-Palmer distribution.

The initial isotopic composition of the ~~decrease became steeper. It reached a minimum value~~ hydrometeor is determined by the surrounding vapour at ~~23 UTC and remained roughly constant thereafter. d_v rose from 5‰ to 20‰ during~~ its initialisation height. By default, formation via the ~~event (Fig. **??**d, black line). A gradual increase~~ Wegener-Bergeron-Findeisen mechanism is assumed between 0 and −23°C. Optionally, a fraction of mass can be added that is formed by ~~about 5‰ before the arrival~~ riming of supercooled cloud droplets on the ~~surface front was followed by~~ hydrometeor (Appendix **??**). The hydrometeor is solid at temperatures below 0°C and melts instantaneously when its temperature exceeds 0°C. Although melting happens over a ~~more rapid 10‰ increase~~ ∼300 m deep layer in reality (Frick et al., 2013), this is a valid assumption considering that hydrometeors start to melt from the ~~4 hours after the frontal passage. A distinct spike of 5‰ in d_v occurred just after~~ outside (Austin and Bemis, 1950) and therefore expose their liquid fraction to the ~~passage of~~ surrounding vapour from the ~~front at 19 UTC. Other short-term variations~~ beginning of ~~d_v occurred within~~ the ~~uncertainty range.~~

~~Now we compare~~ melting process.

3]

Cold frontal passage on 20 November 2015

We now apply the ~~equilibrium vapour~~ framework outlined above to data from ~~precipitation with the~~ a prolonged rainfall period in northern Switzerland. High-resolution rain and vapour isotope measurements ~~to identify the possible influence of below-cloud processes. The isotopic signals of vapour (δ^2H_v; black line~~ reveal variations in ~~Fig. **??**c) and equilibrium vapour from~~ the ~~86 rain samples ($\delta^2H_{p,eq}$; blue bars in Fig. **??**c) exhibit a similar evolution~~ below-cloud processes during the ~~whole~~ event. ~~Differences are overall less than 23‰. $\delta^2H_{p,eq}$ is more variable and its evolution is less smooth than for δ^2H_v. After~~

3.1]

Meteorological situation

The local meteorology of this event was characterised by an ~~initial decrease with a subsequent increase similar to δ^2H_v, $\delta^2H_{p,eq}$ reaches two maxima at around 14 and 16 UTC,~~ extended front over Central Europe, which ~~coincide with low relative humidity and weak rain intensity. It decreases afterwards until~~ was the ~~end~~ remnant of a cold front associated with a decaying cyclone over the ~~sampling period.~~ Gulf of Finland. The ~~decrease is particularly strong~~ nearly zonally oriented front passed Switzerland from a northerly direction during 20 November 2015, before leading to the ~~passage~~ genesis of a new cyclone

over the ~~surface front and during~~ Gulf of Genoa on the ~~second distinct temperature drop (after 20:30 UTC).~~ following day. The ~~overall evolution corresponds~~ rainband associated with the cold front extended zonally over a distance of about 400 km from the Burgundy (France) across Switzerland to the Lake Constance, with a ~~flat W-shape~~ distinct band of high rain intensity (Fig. **??**a). This intense rainband was embedded in a broader zone with stratiform rain. Near Zurich, the ~~first part~~ frontal passage led to a decrease of ~~the event until 16 UTC,~~ equivalent potential temperature (θ_e) at 850 hPa of more than 12 K and to a ~~strong decrease in~~ veering of the ~~second part. This is similar~~ wind from southwest to ~~what found for a cold front~~ northwest (Fig. **??**b).

3.2]

Meteorological surface observations

An overview of selected surface measurements between 06 UTC 20 November and 01 UTC 21 November 2015 is shown in ~~an idealised extratropical cyclone, but~~ Fig. **??**. The local 2-m temperature (T; red line in ~~our case without the increasing branch at the end, which may have occurred~~ Fig. **??**a) remained roughly constant during the ~~not sampled weak rain at the end~~ first part of the ~~event.~~

~~The $d_{\mathrm{p,eq}}$ varies around 0‰~~ event, with a slight increase before 14 UTC. At 19 UTC, ~~and then increases markedly during the passage of~~ when the surface front ~~with values of more than 10‰. Notably, negative values~~ arrived at the measurement location, a rapid drop of ~~$d_{\mathrm{p,eq}}$ occur during periods with weak rain (e.g., around 08:30, 13:30~~ about 2.5°C in 30 min was recorded. The temperature gradually decreased further by about 3.5°C between 20 and ~~16:00 UTC). d_{v} also increases~~ 22 UTC and remained constant thereafter, resulting in an overall decrease in T of ~ 6 K. Local relative humidity at 2 m (h; blue line in Fig. **??**a) varied between $75-85$%before the frontal passage, and increased to values around $85-90\%$ thereafter.

The rain associated with this frontal event started in Zurich at 06 UTC 20 November and lasted until 03 UTC 21 November 2015. Most of the precipitation appeared to be of stratiform nature. The total rain measured by a rain gauge on the rooftop was 30.9 mm, whereof 27.5 mm fell during the ~~event, but less abruptly~~ part of the event investigated here (07:00 - 23:30 UTC). The intensity varied between 0 and 3 mm h^{-1}, before increasing briefly to 10 mm h^{-1} as the surface front passed at 19 UTC (Fig. **??**b). Thereafter, the intensity remained relatively high compared to the period prior to the frontal passage with an average of 3 mm h^{-1} until approximately 23 UTC, when it decreased to low values for the remainder of the event. Between 12 and 18 UTC, sustained wind speeds occurred with values between 5 and 10 m s^{-1}, and therefore the rain intensity is likely underestimated during this period due to the exposed location of the rain gauge. A less ~~variations than $d_{\mathrm{p,eq}}$.~~ exposed meteorological station (MeteoSwiss Station Zurich Fluntern, at a distance of 1.3 km) recorded a total amount of rain of 38.3 mm at 1 m above ground level. For further analysis, we split the event into ~~two periods,~~ a pre-frontal period until about 18:45 UTC ~~(samples~~ (purple shading, precipitation samples 1–54) and a post-frontal ~~one (samples~~ period thereafter (green shading, precipitation samples 55–86).

~~We now briefly consider correlations of~~ According to two balloon soundings launched from the ~~isotope time series with meteorological variables. $d_{p,eq}$ exhibits a positive correlation with h ($\rho = 0.88$) and rain intensity ($\rho = 0.63$). Smaller drops~~ measurement site in Zurich during ~~phases with weak rain and~~ the event, the height of the 0°C isotherm decreased from 2700 m a.s.l. at 16:30 UTC to 1500 m a.s.l. at 22:30 UTC during the frontal passage (not shown).

3.3]

Isotopic composition of vapour and rain

The 10-minute averaged isotope values in surface vapour in Zurich were between $-265‰$ and $-105‰$ for δ^2H_v (Fig. **??**c, black line), and between $-35‰$ and $-14‰$ for $\delta^{18}O_v$ (not shown). The vapour isotope measurements exhibit an overall decrease of more than 160‰ for δ^2H_v during the entire event. A weak decrease in δ^2H_v around 08 UTC was followed by a steady increase until 14 UTC. δ^2H_v decreased thereafter, and the decrease became steeper after 18 UTC, before reaching a roughly constant minimum value at 23 UTC of about $-265‰$. For d_v, values increased from 5‰ to 20‰ during the event (Fig. **??**d, black line). A gradual increase by about 5‰ before the arrival of the surface front was followed by a more rapid 10‰ increase in the 4 h after the frontal passage at about 19 UTC, marked by a distinct spike of 5‰ in d_v. Other short-term variations of d_v were within the uncertainty range (grey shading).

To identify the possible influence of below-cloud processes we now compare the vapour isotope measurements with the precipitation, using the above-defined metric of equilibrium vapour. The isotopic signals of vapour (δ^2H_v; black line in Fig. **??**c) and equilibrium vapour from the 86 rain samples ($\delta^2H_{p,eq}$; blue bars in Fig. **??**c) exhibit a similar evolution during the whole event. Differences are overall less than 23‰. $\delta^2H_{p,eq}$ is more variable and its evolution is less smooth than for δ^2H_v. After an initial decrease with a subsequent increase similar to δ^2H_v, $\delta^2H_{p,eq}$ reaches two maxima at around 14 and 16 UTC, which coincide with low relative humidity and weak rain intensity. It decreases afterwards until the end of the sampling period. The decrease is particularly strong during the passage of the surface front and during the second distinct temperature drop (after 20:30 UTC). The overall evolution corresponds to a flat W-shape in the first part of the event until 16 UTC, and a strong decrease in the second part. This is similar to what Dütsch et al. (2016) found for a cold front in an idealised extratropical cyclone, but in our case without the increasing branch at the end, which may have occurred during weak rain at the end of the event (not sampled).

The $d_{p,eq}$ varies around 0‰ before 19 UTC, and then increases markedly during the passage of the front with values of more than 10‰ (Fig. **??**d). Notably, negative values of $d_{p,eq}$ occur during periods with weak rain (e.g., around 08:30, 13:30 and 16:00 UTC). d_v also increases during the event, but less abruptly and with less variations than for $d_{p,eq}$, which exhibits a positive correlation with h (Spearman $\rho = 0.88$) and rain intensity ($\rho = 0.63$). Smaller drops during phases with weak rain and low relative humidity experience enhanced evaporation, which decreases $d_{p,eq}$.

The similar evolution of δ^2H_v and $\delta^2H_{p,eq}$ in Fig. **??**c indicates that equilibration of rain with the surrounding vapour plays an important role for the evolution of the time series. A principal challenge in identifying the influence of below-cloud processes in joint observations of vapour and precipitation is, however, the dominance of signals from meso-scale meteorological processes, such as the transition between airmasses at the weather front. In order to facilitate the interpretation of these

measurements in terms of below-cloud processes, we introduce in the next sections a new framework that makes the involved physical processes more explicit.

One can also consider the effect of below-cloud processes on ambient vapour. However, on short enough time-scales (a hydrometeor falling from the cloud to the ground), the effect on vapour can be neglected, since the amount of vapour in a given air volume exceeds the amount of liquid or solid by far, especially for the rain rates we measured (for the calculation see Graf (2017)). The effect on vapour would only appear over a longer time period. In the event we present here, a part of the gradual depletion of vapour after 16 UTC could be caused by interaction with falling precipitation or downward motion of the air, which introduces depleted moisture.

It is apparent from Fig. **??**c,d that the difference between vapour isotope measurements and the equilibrium vapour for precipitation varies systematically throughout the precipitation event. Their difference is conveniently quantified by $\Delta\delta$ for δ^2H (Eq. 5), and correspondingly by Δd for δd (Eq. 6). The time series of $\Delta\delta$ for all precipitiation samples from the frontal event varies between -20 permil and 12‰ (Fig. **??**a). For Δd, the time series shows negative values, except for the passage of the front (Fig. **??**b). Some rain samples are in equilibrium with vapour for δ^2H ($\Delta\delta \simeq 0$‰; e.g., at 15 UTC), for d ($\Delta d \simeq 0$‰; at about 19 and 21 UTC) or for both ($\Delta\delta$ and $\Delta d \simeq 0$‰; at 10 UTC). Other samples indicate the influence of below-cloud evaporation with a positive $\Delta\delta$ and a strongly negative Δd (at about 14 and 16 UTC). Most post-frontal samples have a strongly negative $\Delta\delta$ and a Δd close to zero, which indicates the conservation of depleted $\delta^2\mathrm{H}_{\mathrm{p,eq}}$ from the cloud and incomplete equilibration with near-surface vapour. The influence of rain evaporation also results in a negative correlation of $\Delta\delta$ with h ($\rho = -0.65$) and rain intensity ($\rho = -0.44$). The correlation with h is also strong for Δd ($\rho = 0.83$).

4 Idealized simulations with a below-cloud interaction model

The systematic variation of $\Delta\delta$ and Δd throughout the precipitation event motivates us to investigate the influence of meteorological driving factors on these parameters using an idealised model of below-cloud effects (Sec. 2.3). To illustrate the representation of below-cloud processes in this model, we in detail consider the isotopic fractionation of falling precipitation in a set of reference simulations and sensitivity experiments, before transferring the findings to the measurements of the precipitation during 20–21 November 2015.

4.1 Reference simulations

The model configuration consists here of a single-column model domain with a surface pressure of 950 hPa, and extending from 500 m at the surface to 3500 m a.s.l. Time-constant vertical background profiles of temperature T, relative humidity h, $\delta^2\mathrm{H_v}$ and d_v are obtained from the moist adiabatic ascent of an air parcel that is lifted from the surface with initial values of $T_0 = 12°\mathrm{C}$, $h_0 = 0.75$ (Fig. **??**a, green and blue lines). The background isotope profiles are obtained correspondingly from Rayleigh fractionation during a moist adiabatic ascent with an surface composition of $\delta^2\mathrm{H_v} = -150$‰ and $d_\mathrm{v} = 10$‰ (Figs. **??**c,d, solid black lines). Below cloud base (lifting condensation level) at 1030 m a.s.l (dotted horizontal lines), specific humidity and isotopic composition of the vapour are constant, while h increases. Above cloud base, the air parcel follows a Rayleigh

fractionation process. Fractionation increases with decreasing temperature and hence the rate of decrease of $\delta^2\mathrm{H_v}$ becomes more negative with height. The effect of condensation on the profile of d_v (black line in Fig. **??**d) is small at low altitudes and only becomes apparent in the uppermost 500 m of the domain, where d_v starts to increase. Note that this background state of the model is not affected by evaporating droplets or other processed during the simulation.

Now, three hydrometeors representing typical drop sizes for mid-latitude rain are introduced at the formation height at 3500 m a.s.l. The initial diameters (0.56, 1.02 and 2.00 mm) have been calculated iteratively such that the hydrometeors reach target diameters of 0.5, 1 and 2 mm when arriving at the surface. The hydrometeors fall with an average terminal velocity of 2.4, 4.2 and 7.0 $\mathrm{m\,s^{-1}}$, respectively, while growing in supersaturated and shrinking in unsaturated conditions, as expressed by their mass relative to the mass at formation height m/m_init (Fig. **??**b). The saturation of the environment with respect to the hydrometeor depends on the phase and the temperature of the hydrometeor, quantified by the effective relative humidity ~~experience enhanced evaporation, which~~ h_eff of a 1 mm hydrometeor (Fig. **??**a, dotted blue line). The air layer between formation height (3500 m) and the 0°C-isotherm (~ 2250 m) is saturated with respect to liquid water and supersaturated with respect to ice. Therefore, solid hydrometeors grow due to $h_\mathrm{eff} > 100\%$. The growth slows down as h_eff becomes smaller towards the 0°C-isotherm, but continues between the 0°C-isotherm and the cloud base as hydrometeors fall into warmer air and retain a slightly lower temperature than the environment. Finally, the hydrometeors fall into sub-saturated air below the cloud base and start to evaporate. The decreases ~~$d_\mathrm{p,eq}$~~ of m/m_init is fastest for the small hydrometeor (Fig. **??**b, blue line). Evaporation decreases the droplet temperature, which leads to a higher h_eff than h below the cloud base. This effect dampens evaporation by more than 50% compared to a case where the droplet takes on ambient air temperatures.

The initial isotopic composition of the hydrometeors (Fig. **??**c, solid colored lines, symbol A) is enriched by about 100‰ in $\delta^2\mathrm{H}$ compared to the composition of the surrounding vapour (black line). Above the 0°C-isotherm, the hydrometeors are frozen and thus hardly change their isotopic composition (Figs. **??**c,d; A to B). Simulated hydrometeors melt instantaneously when their temperature exceeds 0°C and equilibration sets in, which rapidly changes their isotopic composition towards equilibrium with the surrounding vapour. Comparison between the isotopic composition of the droplets (Figs. **??**c,d, solid coloured lines, symbols A,B,C) and the background vapour is facilitated here by using the equilibrium variables $\delta_\mathrm{p,eq}$ and $d_\mathrm{p,eq}$ (dashed coloured lines, symbols A',B',C'). A drawback of these variables is the discontinuity at the height of the 0°C-isotherm (Figs. **??**c,d, symbol B'). When the hydrometeor changes its state from solid to liquid, the fractionation coefficients change and consequently $\delta_\mathrm{p,eq}$ and $d_\mathrm{p,eq}$ jump.

Hydrometeors equilibrate more quickly the smaller they are, while the 2 mm hydrometeor never reaches equilibrium. Below cloud base, evaporation leads to an enrichment of the small hydrometeors with respect to equilibrium with the surrounding vapour (symbol C´ in **??**c). The ~~correlation~~ hydrometeors' d-excess is smaller than d_v (Fig. **??**d, solid lines at symbol A, black line). Non-equilibrium fractionation due to supersaturation with respect to ice increases d_p compared to d_v (symbol C in Fig. **??**d). The smaller d_p values found here are due to the fact that for strongly depleted vapour, the equilibrium fractionation of $\delta^2\mathrm{H}$ is less than 8 times stronger than that of $\delta^{18}\mathrm{O}$, as discussed in detail by Dütsch et al. (2017).

4.2]

Reference simulations in the $\Delta\delta$ and Δd diagram

We will now cast the results from the idealised model using the variables $\Delta\delta$ and Δd that have been introduced above to measure the deviation of the precipitation from equilibrium with ambient vapour at the surface. To this end, we consider first the $\Delta\delta$ in the reference simulations above for three different rain drops that fall through the atmospheric column (Fig. **??**a). After formation at a height of $z = 3500$ km (colored diamonds), the hydrometeors are depleted by 63‰ in δ^2H (i.e., $\Delta\delta$ is -63‰) compared to surface vapour. As the droplets fall, the $\Delta\delta$ changes little until reaching the melting level (colored triangles). Equilibration above cloud base (coloured crosses) moves them progressively closer to the ambient vapour (black line) and its surface value (black circle). Below cloud base, evaporation in addition introduces fractionation that leads to positive $\Delta\delta$ for the smallest droplet (blue line), whereas the largest droplet has a negative $\Delta\delta$ at the surface, indicating incomplete equilibration, that was not overprinted entirely by the evaporation-induced fractionation.

The initial Δd of -7.5‰ at formation height evolves due to both equilibrium and kinetic fractionation as the droplets fall through the atmospheric column (Fig. **??**b). This leads initially to Δd becoming less negative, reaching equilibrium with ~~h is also strong~~ the ambient vapour for the smallest droplets at cloud base. As the droplets continue to fall through an unsaturated atmosphere below, kinetic fractionation sharply increases Δ ~~d ($\rho = 0.83$). The influence of rain evaporation also results in a negative correlation~~ d, again most markedly for the small droplets, which experience the strongest relative loss of their mass.

When using $\Delta\delta$ ~~with h ($\rho = -0.65$)~~ and ~~rain intensity ($\rho = -0.44$).~~

The similar Δd as the axes of a new diagram, the evolution of ~~δ^2H_v and $\delta^2H_{p,eq}$~~ the droplets in ~~Fig. **??**c indicates that equilibration~~ the three reference simulations yield inverted U-shaped curves (Fig. **??**c). In the examples provided here, these curves depend entirely on the size of the rain ~~with~~ drops at the ~~surrounding vapour plays an important role for~~ surface (large filled dots), placing them either in the ~~evolution~~ lower left quadrant of the ~~time series. In order to facilitate~~ diagram (large drop, comparatively weak below-cloud interaction) or in the ~~interpretation~~ lower right quadrant (small drop, with at first complete equilibration followed by strong below-cloud evaporation). Hence, the location of ~~measurements,~~ a ~~new framework~~ precipitation sample in this $\Delta\delta\Delta d$-diagram is ~~introduced below that makes the different physical~~ determined by several processes ~~more explicit.~~

~~**A new interpretative framework for below-cloud processes**~~

~~From comparing isotope signals in vapour and equilibrium vapour from precipitation, it appears~~ that occur along the ~~difference between the two quantities would enable a more direct interpretation~~ trajectories of ~~different processes. Using the quantities $\Delta\delta$ and Δd (Eq. 6),~~ the ~~data is again displayed as time series (Fig. **??**).~~

Some rain ~~samples~~ drops from their formation until they are ~~in equilibrium with vapour for δ^2H (e.g.,~~ measured at ~~17 UTC), for d (at about 19 and 21 UTC) or for both (at 10 UTC). Other samples indicate~~ the ~~influence~~ surface. The origin of ~~evaporation with a positive $\Delta\delta$ and a strongly negative Δd (at about 14~~ the diagram ($\Delta\delta = 0‰, \Delta d = 0‰$) indicates full equilibrium between vapour and ~~16 UTC). Most post-frontal samples have a strongly negative $\Delta\delta$~~ precipitation. Note that this does not

indicate that the involved vapour and ~~a Δd close to zero, which~~ rain drops did not experience non-equilibrium fractionation processes; it merely indicates that at the ~~conservation~~ time of ~~depleted $\delta^2H_{p,eq}$ from the cloud and incomplete equilibration with near-surface vapour. The identification~~ simultaneously measuring water isotopes in vapour and ~~interpretation~~ rain, the two values correspond to the local equilibrium conditions.

Note that the final locations of ~~these processes from~~ the ~~new parameters~~ droplets' isotopic deviations, $\Delta\delta$ and Δ ~~d is considerably more immediate than from~~ d, in Fig. **??**c correspond to the measured data points shown in Fig. **??**. We now display the measurement data points in the $\Delta\delta\Delta d$-diagram to investigate the ~~time-series of δ^2H_v, $\delta^2H_{p,eq}$, d_v and $d_{p,eq}$.~~

The influence of different below-cloud processes ~~becomes even more apparent when displaying~~ on the ~~data using $\Delta\delta$~~ surface measurements during the frontal passage. By means of additional model sensitivity experiments, we then apply this framework to interpret and ~~Δd as coordinate axes in one diagram (Fig. **??**). The origin~~ quantify the influence of below-cloud effects on the ~~diagram (0,0) indicates full equilibrium between~~ vapour and ~~precipitation. Rain samples of~~ precipitation isotope composition observed at the ~~20 November 2015 event are displayed~~ surface during the frontal passage in November 2015.

5 Observed below-cloud effects in the ~~$\Delta\delta\Delta d$-space, sized by~~ $\Delta\delta\Delta d$-diagram

5.1]

Rain samples during the cold frontal passage

The 86 rain ~~rate in Fig. **??**a and coloured by sample number~~ samples cover a much larger range in ~~Fig. **??**b. Few~~ the $\Delta\delta\Delta d$-diagram than the 3 idealised simulations (Fig. **??**a). Some data points are located in the ~~vicinity of the origin,~~ lower right quadrant, associated with intermediate rain rates (cf. Fig. **??**b) during the pre-frontal phase of the ~~event.~~ event (blue to green shading). Compared to the idealised simulations, these data points match with intermediate to small droplets that experienced evaporation (blue and red dot). Data points located to the left of the origin indicate that precipitation is more depleted than ambient ~~air,~~ vapour, and reflect ~~a stronger cloud~~ that more of the initial signal after formation ("cloud signal") is retained in precipitation. In the idealised experiments, this corresponds to the largest drop size (yellow dot). Most of the post-frontal data points with the most intense rain rates (cf. Fig. **??**b) are located to the left of the ~~origin. The data points seem to follow a line with a negative slope. A linear fit through the samples yields a regression line with a slope of $\frac{\Delta d}{\Delta\delta} = -0.31$ (Fig. **??**a, solid black line). Rain falling through unsaturated air will lead~~ origin (orange to ~~an increase in $\Delta\delta$ and a decrease in Δd.~~

~~It is noteworthy that similar slopes (-0.30 ± 0.02; dashed black lines in Fig. **??**a) were found for three other cold fronts in Switzerland . This indicates that the slope may represent general characteristics of below-cloud evaporation~~ red shading).

Drop size, and ~~equilibration of rainfall during continental mid-latitude cold fronts.~~

~~Overall, the~~ thus rain rate ~~strongly influences~~ appears as an important driving factor of the ~~location~~ below-cloud processes. Figure **??**b shows another variant of the ~~samples in~~ $\Delta\delta\Delta d$-diagram where the ~~diagram. Samples~~ dot size indicates rain rate.

It appears that samples with the highest rain rates are located in the upper left corner, as they are ~~less~~ least affected by below-cloud processes and retain more of their initial strongly negative $\Delta\delta$. Samples from periods with weak rain rates are located in the bottom right corner of the diagram, reflecting a stronger evaporation influence. ~~In comparison, the influence of~~ Overall, complete equilibration ~~is weaker than of evaporation, which is indicated by the low number of~~ with ambient vapour seems to be rather limited because only few data points are close to the origin of the diagram. The regions in Fig. **??**a that are covered by pre-frontal (purple) and post-frontal (green) samples are fairly well separated. ~~This indicates that pre-frontal~~ Pre-frontal samples, which are on average higher in $\Delta\delta$ and lower in Δd, ~~are~~ seem to be more strongly affected by below-cloud processes than post-frontal samples. ~~The~~ From the idealised model experiments, such a difference can be explained by an on average lower rain intensity and a lower relative humidity during the pre-frontal phase, and therefore by enhanced below-cloud equilibration and evaporation. Additionally, the melting layer was clearly lower after the passage of the front, and thus both vertical distance and ~~time for~~ time for equilibration were reduced. Post-frontal samples therefore carry more of their depleted initial $\delta^2\mathrm{H}_{\mathrm{p,eq}}$ from the cloud base to the surface.

The data points in Fig. **??** roughly fall along a line with a negative slope. A linear fit through the samples yields a regression line with a slope of $\frac{\Delta d}{\Delta \delta} = -0.31$ (Fig. **??**b, solid black line). It is noteworthy that similar slopes (-0.30 ± 0.02; dashed black lines in Fig. **??**b) were found for three other cold fronts in Switzerland (Graf, 2017). This indicates that the slope could represent a general characteristic of below-cloud evaporation and equilibration ~~were reduced. Post-frontal samples therefore carry more of their depleted initial $\delta^2\mathrm{H}_{\mathrm{p,eq}}$ from the cloud~~ rainfall, at least for continental mid-latitude cold front passages. It will be insightful to explore the ~~ground.~~ slope in the $\Delta\delta\Delta d$-diagram for other climatic regions in future studies.

It is important to ~~note~~ recall that ~~also other meteorological factors influence~~ the isotopic evolution of sedimenting ~~raindrops,~~ rain drops is strongly influenced by ambient meteorological conditions, in particular the detailed relative humidity profile, the formation height of precipitation, the isotope profile of vapour, and potential up- and downdrafts and turbulent motions below the cloud base. The effect of some of these processes ~~can be~~ is now investigated ~~by considering measurements from different rainfall events, and, in particular,~~ with the aid of the idealised below-cloud interaction ~~models. Such an analysis will be presented in a forthcoming paper.~~

~~From the analysis of~~ model, providing further insight to the ~~rainfall and vapour isotopes~~ interpretation of our measurements in the ~~event on 20 November 2015, it appears that presenting data~~ $\Delta\delta\Delta d$-diagram.

5.2 Sensitivity experiments in the ~~$\Delta\delta\Delta d$-space provides an insightful viewing device to decipher~~ $\Delta\delta\Delta d$-diagram

We now use the ~~complexity of~~ below-cloud ~~processes. In the next section, these findings are discussed in more general terms.~~

~~**The influence of evaporation and equilibration**~~

~~A $\Delta\delta\Delta d$-diagram shows the isotopic composition of equilibrium vapour from precipitation samples relative~~ interaction model to assess the relevance of different ambient ~~surface vapour at the time when~~ conditions for the ~~samples were taken. The location of a precipitation sample~~ rain drop trajectories and surface arrival points in the ~~$\Delta\delta\Delta d$-space is determined by two factors: (i)~~ $\Delta\delta\Delta d$-diagram. Explored parameters include the ~~initial composition of precipitation after~~ sensitivity to surface relative humidity, surface temperature, formation ~~in the cloud~~ height, riming, and ~~(ii)~~ the ~~modification~~ background isotope profiles in terms of ~~this composition below the cloud by equilibration~~ δ^2H and ~~evaporation. These below-cloud processes depend on the rain intensity: larger drops during intense rain are typically less affected by below-cloud processes because they spend less time~~ d (as described in ~~the air due to a faster fall velocity and they are more resilient to exchanges with the ambient vapour due to~~ detail in Graf (2017)). For each parameter, several simulations were performed for a ~~smaller surface to volume ratio. The isotopic composition~~ range of drop sizes from 0.6 to 1.8 mm. Assuming a standard Marshall-Palmer dropsize distribution, these diameters correspond to the mass-weighted mean diameter for rain ~~sample is~~ intensities in the range from 0.1 to 20 $\mathrm{mm\,h^{-1}}$.

For a ~~mass weighted average~~ particular setup of the ~~composition of all~~ ambient parameters, the different $\Delta\delta$ and Δd when the drops ~~contained in a sample. The processes that act on a single drop~~ arrive at the surface are ~~thus directly relevant for bulk precipitation.~~

~~The initial $\Delta\delta$ of a precipitating hydrometeor is strongly negative, because it is formed aloft from vapour that is depleted~~ connected by dashed lines in ~~δ^2H compared~~ Fig. **??**. The black line shows the reference experiment (REF, cf. Sec. 4.2), where the filled circle corresponds to ~~vapour at~~ the ~~surface.~~ highest rain intensity, and the triangle to the lowest. The ~~initial Δd~~ label of ~~precipitation~~ the experiments points to the input parameter that is ~~uncertain, but assumed~~ modified. RH50 and RH100 correspond to ~~be small. The increase of d_v~~ sensitivity experiments with ~~height~~ different surface relative humidity $h_0 = 50\%$ and ~~non-equilibrium effects during precipitation~~ $h_0 = 100\%$, respectively. T7 and T17 denote experiments with different surface temperatures $T_0 = 7°\mathrm{C}$ and $T_0 = 17°\mathrm{C}$, FH2.5 and FH5.0 refer to experiments with formation heights of 2.5 km and 5.0 km a.s.l., respectively, and RIM corresponds to formation ~~in mixed-phase clouds, both increase $d_\mathrm{p,eq}$ (and Δd). This increase is however counteracted~~ by ~~a decrease~~ riming. Experiments with altered background profiles of ~~$d_\mathrm{p,eq}$ during~~ stable water isotopes are denoted as $\delta \pm 50$ ($\delta^2\mathrm{H_v}$ profile changed by $\pm 50‰$ above the ~~vapour-solid transition~~ cloud base) and $d \pm 10$ (d_v profile changed ~~by a decrease due to~~ $\pm 10‰$ above the ~~non-linearity~~ cloud base).

Changes of the ~~δ-scale.~~

~~Falling rain adopts~~ model input parameters systematically affect the ~~subsequently enriched δ^2H~~ position and orientation of the ~~surrounding vapour through equilibration. If equilibration~~ curves in the $\Delta\delta\Delta d$-diagram. The results for simulations where the initial composition of hydrometeors is ~~efficient (light rain),~~ modified (T7, T17, FH2.5, FH5.0, RIM, $\delta \pm 50$ and $d \pm 10$) diverge for strong rain intensities. For small drops, i.e., weak precipitation intensities, however, the ~~isotopic difference~~ results converge and are quite similar for all simulations. This agrees with the finding from the reference simulations that below-cloud interaction affects samples from weak rain more strongly and overwrites initial differences. Simulations that alter the extent of below-cloud interaction (RH50, RH100 and to ~~the surrounding vapour becomes~~ a small ~~and rain exhibits~~ degree also T7)

show large differences for small ~~absolute~~ drops. For example, evaporation in RH50 shifts isotope values ~~of~~ in small drops to high $\Delta\delta$ and low Δ ~~d when it arrives at the ground. Strongly equilibrated samples are thus located close to~~ d. In contrast, the ~~origin (0,0)~~ absence of evaporation in ~~Fig. **??**. If~~ RH100 leads to an almost complete equilibration ~~is not efficient (intense rain),~~ with the ambient vapour and almost no change of d. Large drops, representative of strong rain ~~retains more~~ intensities, carry a stronger imprint of ~~its~~ the different initial ~~low δ^2H and arrives at~~ composition of precipitation to the ~~ground~~ surface. Therefore, the coloured dots from simulations with a ~~negative $\Delta\delta$. Weakly equilibrated samples~~ low initial δ^2H (T7, FH5.0, $\delta - 50$) are ~~thus typically~~ located at lower $\Delta\delta$ than simulations with a high initial δ^2H (T17, FH2.5, $\delta + 50$). The same is the case for Δd in simulations where the ~~upper left of Fig. **??**.~~ initial d differs.

The ~~preferential loss of light isotopes and non-equilibrium effects during evaporation~~ set of ~~rain will increase $\delta^2H_{p,eq}$ (and $\Delta\delta$) and decrease $d_{p,eq}$ (and Δd). Rain samples~~ idealized simulations reveals that ~~are strongly affected~~ the closer a precipitation sample is to the origin of the coordinate system, the more it has equilibrated with ambient vapour until it reaches the ground, while remaining unaffected by evaporation. Samples that encountered significant evaporation ~~will thus be~~ during their fall are located ~~in~~ towards the bottom right ~~quadrant~~ of the ~~$\Delta\delta\Delta$~~ $\Delta\delta\Delta$ d-diagram. This is typically the case for samples from weak rain intensities. Samples that were weakly influenced by equilibration or evaporation during their fall, which is typically the case for intense precipitation, are located towards the left side of the diagram. Assuming constant ambient conditions, variations of the rain intensity cause variations in the $\Delta\delta\Delta d$-diagram along a curve as indicated in Fig. **??**. The location and orientation of ~~a sample~~ this curve in this diagram is determined by the meteorological conditions. Studying the evolution of precipitation samples in the ~~$\Delta\delta\Delta d$-space therefore contains~~ $\Delta\delta\Delta d$-diagram during a rain event can thus clearly reveal information about the ~~intensity~~ prevailing meteorological conditions and ~~type of below-cloud processes, because they act differently on the isotopic composition of rain.~~ their temporal evolution.

6 Conclusions

The processes acting on precipitation as it falls from the cloud base to the surface are complex and difficult to ~~access.~~ access from surface measurements only. Using highly resolved measurements of stable isotopes in vapour and rain at the surface, we show here that it is possible to identify an integrated signal of these so-called below-cloud processes ~~using~~ when comparing the isotopic composition of equilibrium vapour from precipitation relative to near-surface vapour simultaneously for both δ^2H and d.

We combine this information in a new interpretation framework, the $\Delta\delta\Delta d$-diagram, where $\Delta\delta$ is shown along the x-axis and Δd along the y-axis. This combines a view of δ^2H_v, $\delta^2H_{p,eq}$, d_v and $d_{p,eq}$ while tuning down the influence of first-order advection processes during a frontal transition. To display data in the $\Delta\delta\Delta d$-diagram, the isotopic composition of surface vapour and precipitation have to be known, as well as surface temperature.

A $\Delta\delta\Delta d$-diagram shows the isotopic composition of equilibrium vapour from precipitation samples relative to the ambient surface vapour at the time when the samples were taken. By means of idealised below-cloud interaction model simulations, we show that the location of a precipitation sample in the $\Delta\delta\Delta d$-space is determined by two factors: (i) the initial composition

of precipitation after formation in the cloud and (ii) the modification of this composition below the cloud by equilibration and evaporation. These below-cloud processes depend on the rain intensity: larger drops during intense rain are typically less affected by below-cloud processes because they spend less time in the air due to a faster fall velocity and they are less affected by exchanges with the ambient vapour due to a smaller surface to volume ratio. The isotopic composition of a ~~new interpretation framework. The $\Delta\delta\Delta d$-diagram~~ rain sample is ~~proposed as~~ a ~~valuable means of displaying measurement data (or model data)~~ mass weighted average of ~~both δ^2H and d simultaneously. It shows~~ the ~~isotopic~~ composition of ~~equilibrium vapour from precipitation relative to near-surface vapour. $\Delta\delta$ is shown along the x-axis and Δd along the y-axis, which combines δ^2H_v, $\delta^2H_{p,eq}$, d_v and $d_{p,eq}$~~ all drops contained in a sample. The processes that act on a single ~~diagram. To display data in the $\Delta\delta\Delta d$-space, the isotopic composition of surface vapour and precipitation have to be known, as well as surface temperature to calculate $\delta^2H_{p,eq}$ and $d_{p,eq}$.~~ drop are thus directly relevant for bulk precipitation. The usefulness of this diagram ~~has been illustrated~~ is demonstrated with measurements from a cold frontal rain event in ~~Switzerland.~~ Switzerland in November 2015.

The main conclusions from this study are:

1. Equilibration between vapour and rain and evaporation of rain in unsaturated air leave distinct imprints in the isotope signal of surface rain. Both aspects of the ~~molecular~~ exchange between the liquid and solid phase become more accessible by quantifying the deviation from isotopic equilibrium with the surface vapour ~~with~~ by studying the two quantities $\Delta\delta$ and Δd.

2. The $\Delta\delta\Delta d$-diagram facilitates the interpretation of the ~~effect~~ effects of below-cloud processes on rain samples by jointly displaying the degree of equilibration between rain and vapour and the influence of evaporation using the newly defined variables $\Delta\delta$ and Δd. Equilibration and evaporation have different pathways in the $\Delta\delta\Delta d$-space, ~~where they are~~ d-diagram, which makes them more easily distinguishable than in a time series. Investigating rain samples in the $\Delta\delta\Delta d$-space ~~is~~ d-diagram can therefore ~~complementary to~~ complement a ~~time series perspective, in particular when data points are further coloured or sized using additional parameters, such as rainfall rate.~~ time-series perspective.

3. ~~Samples from~~ During the 20 November 2015 cold ~~front show that~~ frontal rainfall event evaporation ~~is~~ appears as the dominant ~~process, while equilibration without~~ below-cloud process regarding the isotopic composition of surface rain. The effect of evaporation ~~appears as an exception. Evaporation~~ on the isotope composition is strongly ~~related to~~ modulated by the rain ~~rate, which was less~~ rate. The pre-frontal period with weaker rainfall therefore experienced a stronger signal of evaporation below cloud base, whereas the more intense ~~during~~ post-frontal rainfall contained a stronger signal from the ~~pre-frontal period. Post-frontal samples are less equilibrated and evaporated than pre-frontal samples,~~ cloud level. The cloud signal was also more preserved due to higher below-cloud relative ~~humidity~~ humidity, and a lower temperature and melting layer after the frontal passage.

4. ~~Evaporation causes data points in~~ In the $\Delta\delta\Delta$~~d-space~~ d-diagram, below-cloud processes caused precipitation measurements to follow a line with a negative slope of $\frac{\Delta d}{\Delta \delta} = -0.31$. Similar slopes were obtained for several other frontal rain events, suggesting that the characteristics of below-cloud processes, as revealed by the $\Delta\delta\Delta d$-diagram are similar for this ~~kind~~ type of cold frontal rain ~~events.~~ events in continental mid-latitudes.

Using the $\Delta\delta\Delta d$ framework, it will be highly valuable to investigate ~~the~~ below-cloud effects for other precipitation events. For example, a snowfall event, or a transition from rain to snow could show a stronger cloud signal due to the absent exchange between vapour and solid. Cases of drizzle could exhibit a large degree of equilibration between small drops and ambient vapour. Cases of convective rainfall could show variations ~~between~~ due to more cloud-related signals in ~~downdrafts~~ convective downdrafts.

Further constraints on observations from radiosondes, vertically resolved isotope measurements using aircraft (e.g., Dyroff et al., 2015; Sodemann et al., 2017) and ~~stronger evaporation~~ related measurements at high resolution will provide possibilities to validate and ~~equilibration in updrafts.~~ apply the idealised modelling framework presented here for below-cloud processes.

We expect that the analysis of the isotopic composition during rain events at other locations and further model studies will benefit from using the parameters $\Delta\delta$ and Δd, and the $\Delta\delta\Delta d$-diagram as an additional viewing device to obtain insight into below-cloud processes. Thereby, further constraints on microphysical processes in models can be obtained, and ultimately contribute to a more complete use of stable water isotopes to build internally consistent water cycles into numerical weather prediction and climate models.

References

Aemisegger, F.: Atmospheric stable water isotope measurements at the timescale of extratropical weather systems, Ph.D. Thesis, ETH No. 21165, ETH Zurich, 2013.

Aemisegger, F., Sturm, P., Graf, P., Sodemann, H., Pfahl, S., Knohl, A., and Wernli, H.: Measuring variations of δ18O and δ2H in atmospheric water vapour using two commercial laser-based spectrometers: an instrument characterisation study, Atmos. Meas. Tech., 5, 1491–1511, https://doi.org/10.5194/amt-5-1491-2012, 2012.

Aemisegger, F., Spiegel, J. K., Pfahl, S., Sodemann, H., Eugster, W., and Wernli, H.: Isotope meteorology of cold front passages: A case study combining observations and modeling, Geophys. Res. Lett., 42, 5652–5660, https://doi.org/10.1002/2015GL063988, 2015.

Austin, P. M. and Bemis, A. C.: A quantitative study of the "bright band" in radar precipitation echoes, J. Meteor., 7, 145—151, 1950.

Barras, V. and Simmonds, I.: Observation and modeling of stable water isotopes as diagnostics of rainfall dynamics over southeastern Australia, J. Geophys. Res. Atmos., 114, D23 308, https://doi.org/10.1029/2009JD012132, 2009.

Bennett, L. J., Browning, K. A., Blyth, A. M., Parker, D. J., and Clark, P. A.: A review of the initiation of precipitating convection in the United Kingdom, Q. J. R. Meteorol. Soc., 132, 1001–1020, https://doi.org/10.1256/qj.05.54, 2007.

Celle-Jeanton, H., Gonfiantini, R., Travi, Y., and Sol, B.: Oxygen-18 variations of rainwater during precipitation: application of the Rayleigh model to selected rainfalls in Southern France, J. Hydrol., 289, 165–177, https://doi.org/10.1016/j.jhydrol.2003.11.017, 2004.

Ciais, P. and Jouzel, J.: Deuterium and oxygen 18 in precipitation: Isotopic model, including mixed cloud processes, J. Geophys. Res. Atmos., 99, 16 793–16 803, https://doi.org/10.1029/94JD00412, 1994.

Cooney, J.: Remote measurements of atmospheric water vapor profiles using the Raman component of laser backscatter, J. Appl. Meteor., 9, 182–184, 1970.

Coplen, T. B., Neiman, P. J., White, A. B., Landwehr, J. M., Ralph, F. M., and Dettinger, M. D.: Extreme changes in stable hydrogen isotopes and precipitation characteristics in a landfalling Pacific storm, Geophys. Res. Lett., 35, L21 808, https://doi.org/10.1029/2008GL035481, 2008.

Dansgaard, W.: The O 18-abundance in fresh water, Geochim. Cosmochim. Ac., 6, 241–260, https://doi.org/10.1016/0016-7037(54)90003-4, 1954.

Dansgaard, W.: Stable isotopes in precipitation, Tellus, 16, 436–468, 1964.

Dütsch, M., Pfahl, S., and Wernli, H.: Drivers of δ2H variations in an idealized extratropical cyclone, Geophys. Res. Lett., 43, 5401–5408, https://doi.org/10.1002/2016GL068600, 2016.

Dütsch, M., Pfahl, S., and Sodemann, H.: The impact of nonequilibrium and equilibrium fractionation on two different deuterium excess definitions, J. Geophys. Res. Atmos., 122, 12,732–12,746, https://doi.org/10.1002/2017JD027085, 2017.

Dyroff, C., Sanati, S., Christner, E., Zahn, A., Balzer, M., Bouquet, H., McManus, J. B., González-Ramos, Y., and Schneider, M.: Airborne in situ vertical profiling of HDO / $H^{16}O$ in the subtropical troposphere during the MUSICA remote sensing validation campaign, Atmos. Meas. Tech., 8, 2037—2049, https://doi.org/10.5194/amt-8-2037-2015, 2015.

Frick, C., Seifert, A., and Wernli, H.: A bulk parametrization of melting snowflakes with explicit liquid water fraction for the COSMO model, Geosci. Model Dev., 6, 1925—1939, https://doi.org/10.5194/gmd-6-1925-2013, 2013.

Galewsky, J., Steen-Larsen, H. C., Field, R. D., Worden, J., Risi, C., and Schneider, M.: Stable isotopes in atmospheric water vapor and applications to the hydrologic cycle, Rev. Geophys., 54, 409–465, https://doi.org/10.1002/2015RG000512, 2016.

Graf, P.: The effect of below-cloud processes on short-term variations of stable water isotopes in surface precipitation, Ph.D. Thesis, ETH No. 24777, ETH Zurich, https://doi.org/10.3929/ethz-b-000266387, 2017.

IAEA: Reference sheet for international measurement standards VSMOW2 and SLAP2, Int. At. Energy Agency IAEA Vienna, 2009.

Lee, J.-E. and Fung, I.: "Amount effect" of water isotopes and quantitative analysis of post-condensation processes, Hydrol. Process., 22, 1–8, https://doi.org/10.1002/hyp.6637, 2008.

Majoube, M.: Fractionnement en oxygène 18 et deutérium entre l'eau et sa vapeur, J. Chim. Phys., 68, 1423–1436, 1971.

Managave, S. R., Jani, R. A., Rao, T. N., Sunilkumar, K., Satheeshkumar, S., and Ramesh, R.: Intra-event isotope and raindrop size data of tropical rain reveal effects concealed by event averaged data, Clim. Dyn., 47, 981–987, https://doi.org/10.1007/s00382-015-2884-7, 2016.

Miyake, Y., Matsubaya, O., and Nishihara, C.: An isotopic study on meteoric precipitation, Pap. Meteorol. Geophys., 19, 243–266, 1968.

Muller, C. L., Baker, A., Fairchild, I. J., Kidd, C., and Boomer, I.: Intra-event trends in stable isotopes: Exploring midlatitude precipitation using a vertically pointing micro rain radar, J. Hydrometeor., 16, 194–213, https://doi.org/10.1175/JHM-D-14-0038.1, 2015.

Pfahl, S., Wernli, H., and Yoshimura, K.: The isotopic composition of precipitation from a winter storm – A case study with the limited-area model COSMOiso, Atmos. Chem. Phys., 12, 1629–1648, https://doi.org/10.5194/acp-12-1629-2012, 2012.

Risi, C., Bony, S., Vimeux, F., Chong, M., and Descroix, L.: Evolution of the stable water isotopic composition of the rain sampled along Sahelian squall lines, Q. J. R. Meteorol. Soc., 136, 227–242, https://doi.org/10.1002/qj.485, 2010.

Roberts, A. and Knippertz, P.: Haboobs: convectively generated dust storms in West Africa, Weather, 67, 311–316, https://doi.org/10.1002/wea.1968, 2012.

Schneider, M. and Hase, F.: Ground-based FTIR water vapour profile analyses, Atmos. Meas. Tech., 2, 609–619, https://doi.org/10.5194/amt-2-609-2009, 2009.

Seity, Y., Brousseau, P., Malardel, S., Hello, G., Bénard, P., Bouttier, F., Lac, C., and Masson, V.: The AROME-France convective-scale operational model, Mon. Wea. Rev., 139, 976–991, https://doi.org/10.1175/2010MWR3425.1, 2010.

Skamarock, C., Klemp, B., Dudhia, J., Gill, O., Barker, D., Duda, G., Huang, X.-Y., Wang, W., and Powers, G.: A description of the advanced research WRF version 3, NCAR Tech. Note NCARTN-475STR, https://doi.org/10.5065/D68S4MVH, 2008.

Sodemann, H., Aemisegger, F., Pfahl, S., Bitter, M., Corsmeier, U., Feuerle, T., Graf, P., Hankers, R., Hsiao, G., Schulz, H., Wieser, A., and Wernli, H.: The stable isotopic composition of water vapour above Corsica during the HyMeX SOP1 campaign: Insight into vertical mixing processes from lower-tropospheric survey flights, Atmos. Chem. Phys., 17, 6125–6151, https://doi.org/10.5194/acp-17-6125-2017, 2017.

Solheim, F., Godwin, J. R., Westwater, E. R., Han, Y., Keihm, S. J., Marsh, K., and Ware, R.: Radiometric profiling of temperature, water vapor and cloud liquid water using various inversion methods, Radio Sci., 33, 393–404, https://doi.org/10.1029/97RS03656, 1998.

Steppeler, J., Doms, G., Schättler, U., Bitzer, H. W., Gassmann, A., Damrath, U., and Gregoric, G.: Meso-gamma scale forecasts using the nonhydrostatic model LM, Meteorol. Atmos. Phys., 82, 75–96, https://doi.org/10.1007/s00703-001-0592-9, 2003.

Stewart, M. K.: Stable isotope fractionation due to evaporation and isotopic exchange of falling waterdrops: Applications to atmospheric processes and evaporation of lakes, J. Geophys. Res., 80, 1133–1146, https://doi.org/10.1029/JC080i009p01133, 1975.

Wang, S., Zhang, M., Che, Y., Zhu, X., and Liu, X.: Influence of below-cloud evaporation on deuterium excess in precipitation of arid Central Asia and its meteorological controls, J. Hydrometeor., 17, 1973–1984, https://doi.org/10.1175/JHM-D-15-0203.1, 2016.

Xie, X., Evaristo, R., Troemel, S., Saavedra, P., Simmer, C., and Ryzhkov, A.: Radar observation of evaporation and implications for quantitative precipitation and cooling rate estimation, J. Atmos. Oceanic Technol., 33, 1779–1792, https://doi.org/10.1175/JTECH-D-15-0244.1, 2016.

Yoshimura, K., Kanamitsu, M., and Dettinger, M.: Regional downscaling for stable water isotopes: A case study of an atmospheric river event, J. Geophys. Res. Atmos., 115, D18 114, https://doi.org/10.1029/2010JD014032, 2010.